

Supporting Information

**Isomer sensitive electrochemical HER of ruthenium(II)-hydrido complexes
involving redox active azoheteroaromatics**

Liton Seikh,^a Suman Dhara,^a Ajit Kumar Singh,^b Aditi Singh,^a Sanchaita Dey,*^a Arindam Indra*^b and Goutam Kumar Lahiri*^a

^a*Department of Chemistry, Indian Institute of Technology Bombay, Powai, Mumbai-400076, India*

^b*Department of Chemistry, Indian Institute of Technology (BHU), Varanasi, Uttar Pradesh-221005, India*

Email: lahiri@chem.iitb.ac.in(G.K.L)

arindam.chy93@iitbhu.ac.in(A.I)

sanchaitadey93@gmail.com(S.D)

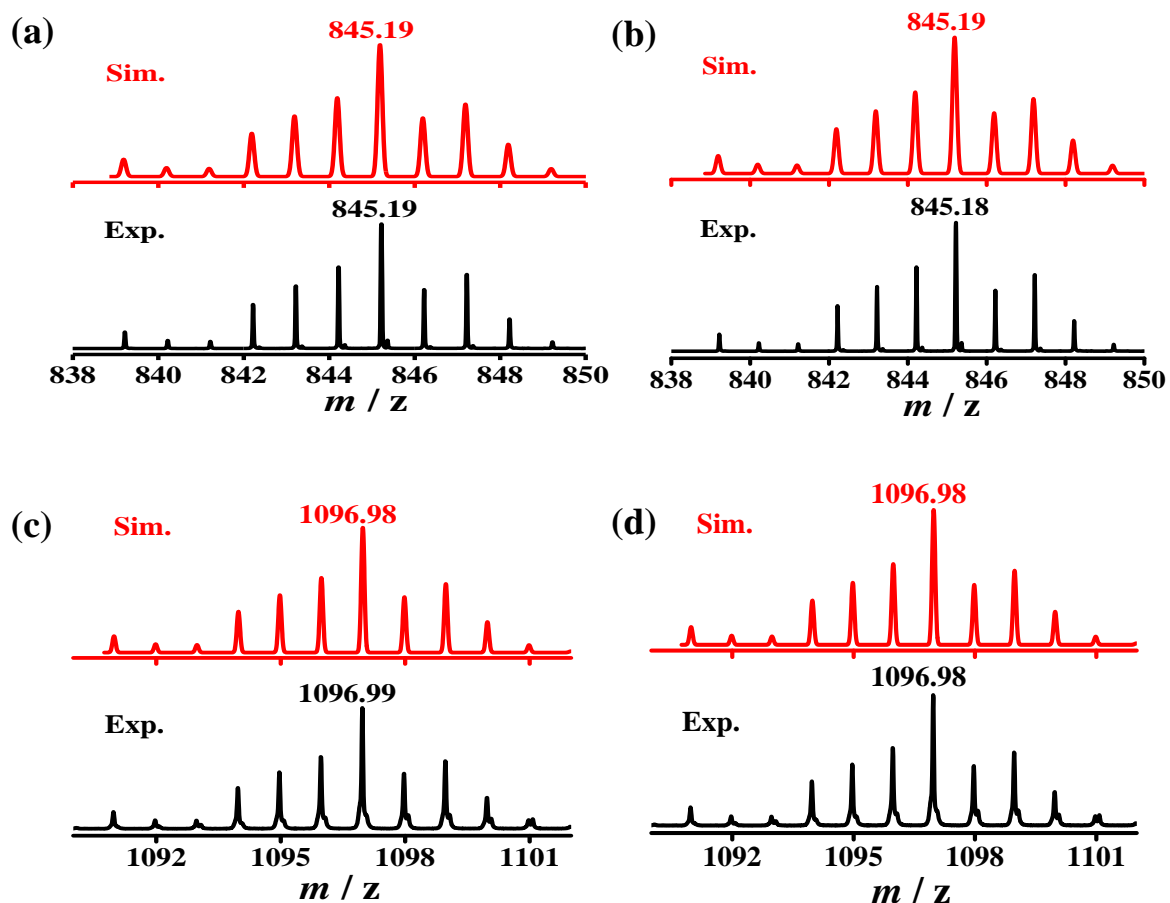


Fig. S1 Experimental and simulated ESI(+) mass of (a) $\{[1\mathbf{a}]\text{ClO}_4\text{-}\text{ClO}_4\}^+$, (b) $\{[1\mathbf{b}]\text{ClO}_4\text{-}\text{ClO}_4\}^+$, (c) $\{[2\mathbf{a}]\text{ClO}_4\text{-}\text{ClO}_4\}^+$ and (d) $\{[2\mathbf{b}]\text{ClO}_4\text{-}\text{ClO}_4\}^+$ in CH_3CN (red line, simulated and black line, experimental).

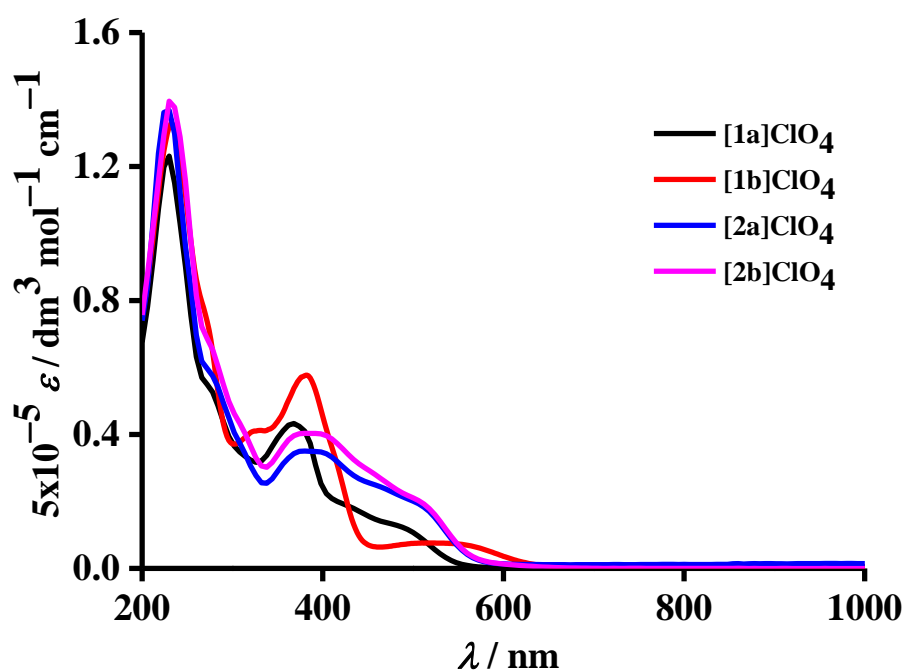


Fig. S2 Electronic spectra of **[1a]** ClO_4 , **[1b]** ClO_4 , **[2a]** ClO_4 and **[2b]** ClO_4 in CH_3CN .

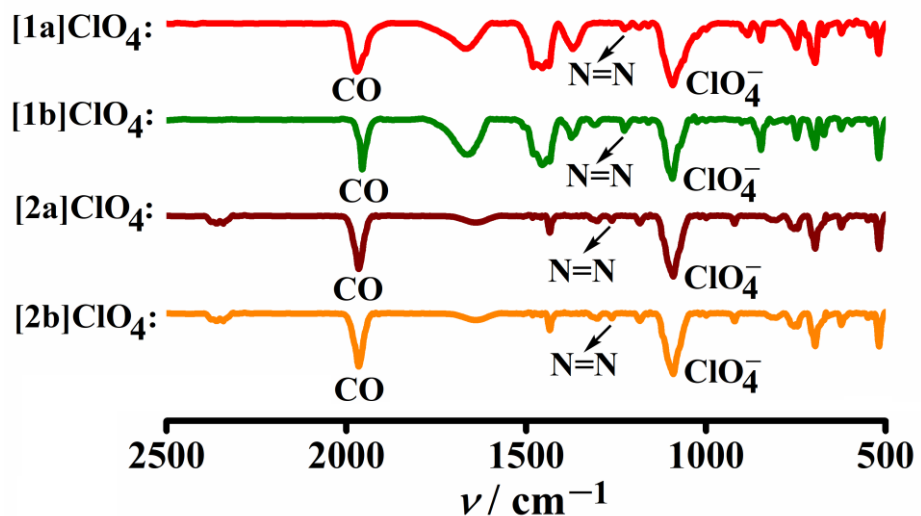


Fig. S3 FT-IR spectra as KBr pellets.

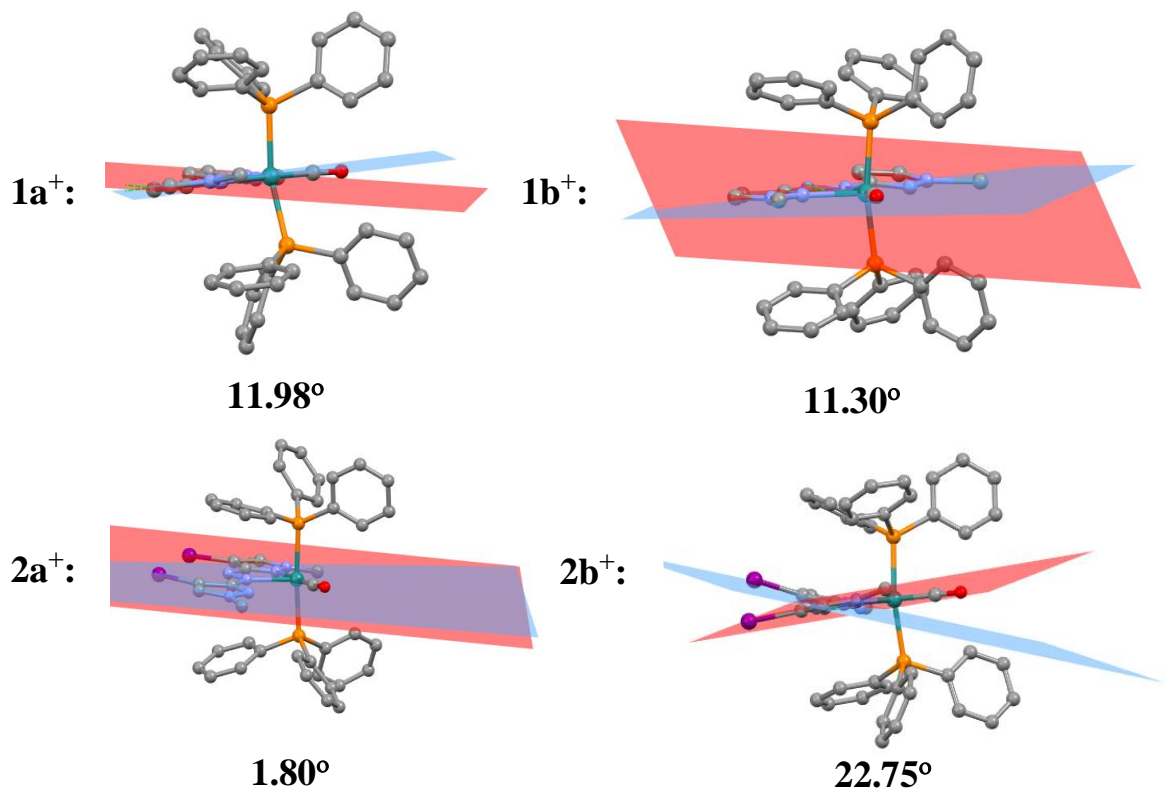


Fig. S4 Non-planarity of the coordinated L1 and L2.

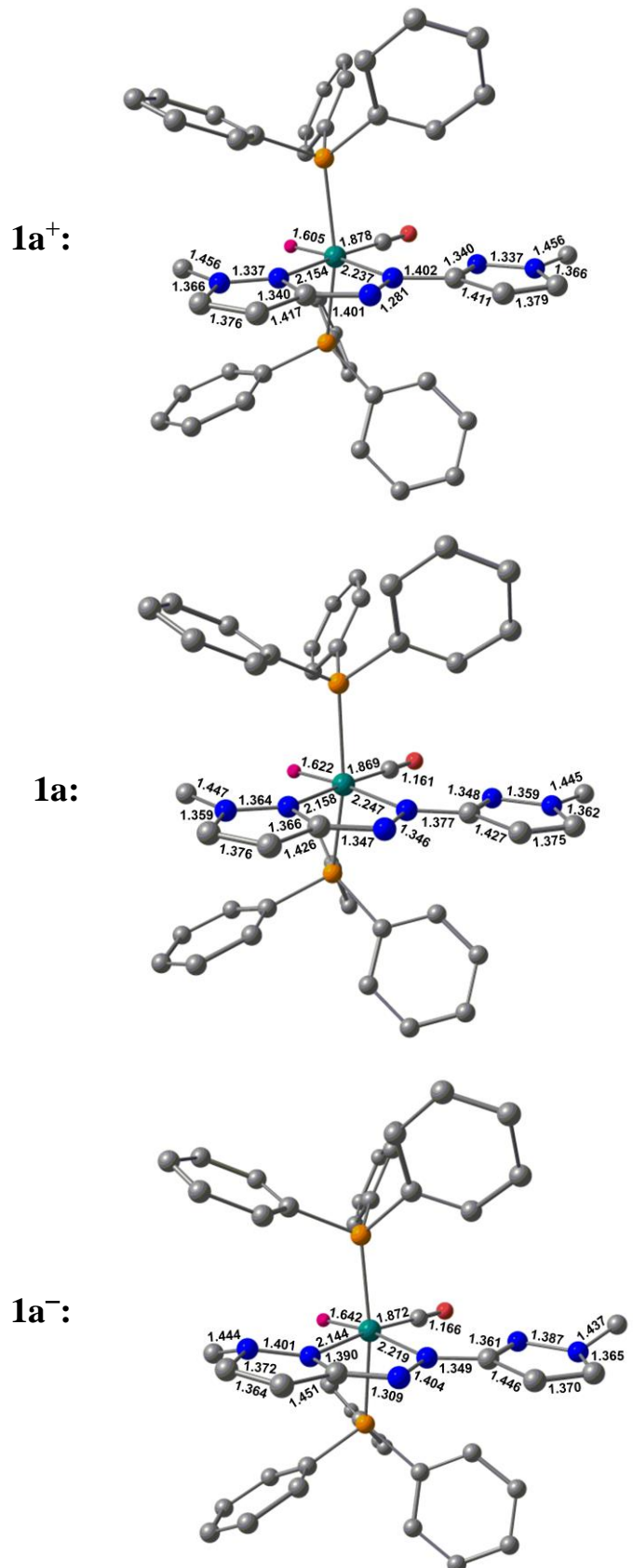


Fig. S5a DFT optimised structures of $\mathbf{1a}^n$ ($n = +1, 0, -1$).

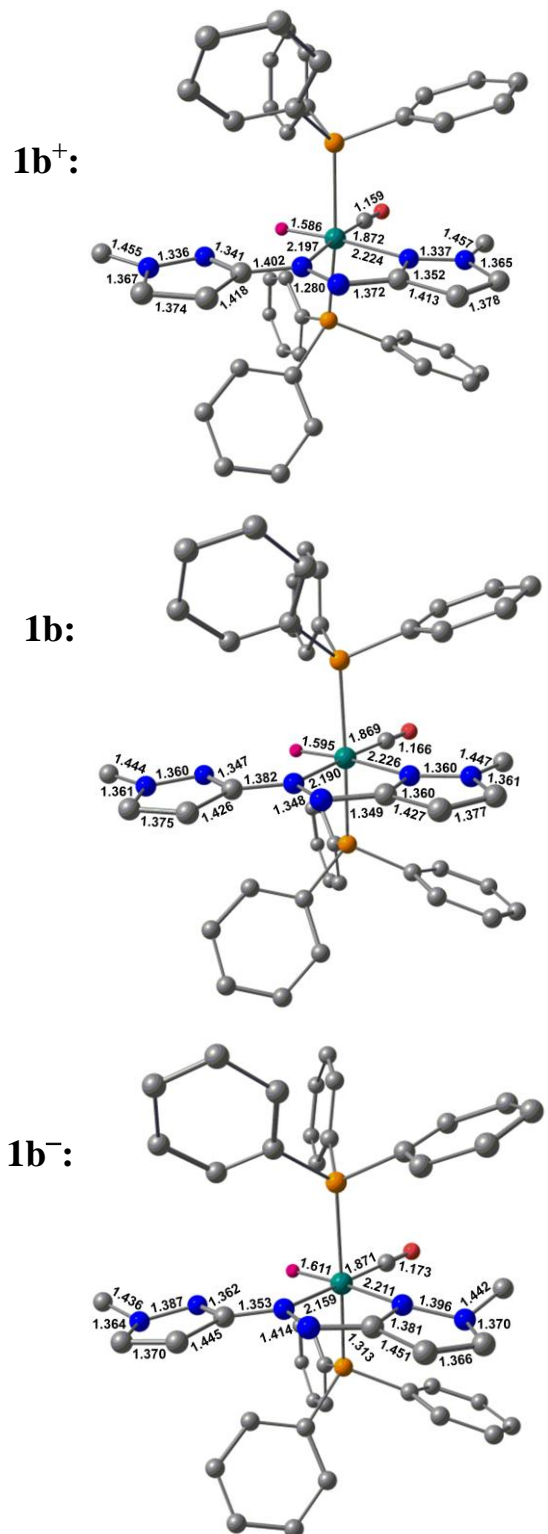


Fig. S5b DFT optimised structures of $\mathbf{1b}^n$ ($n = +1, 0, -1$).

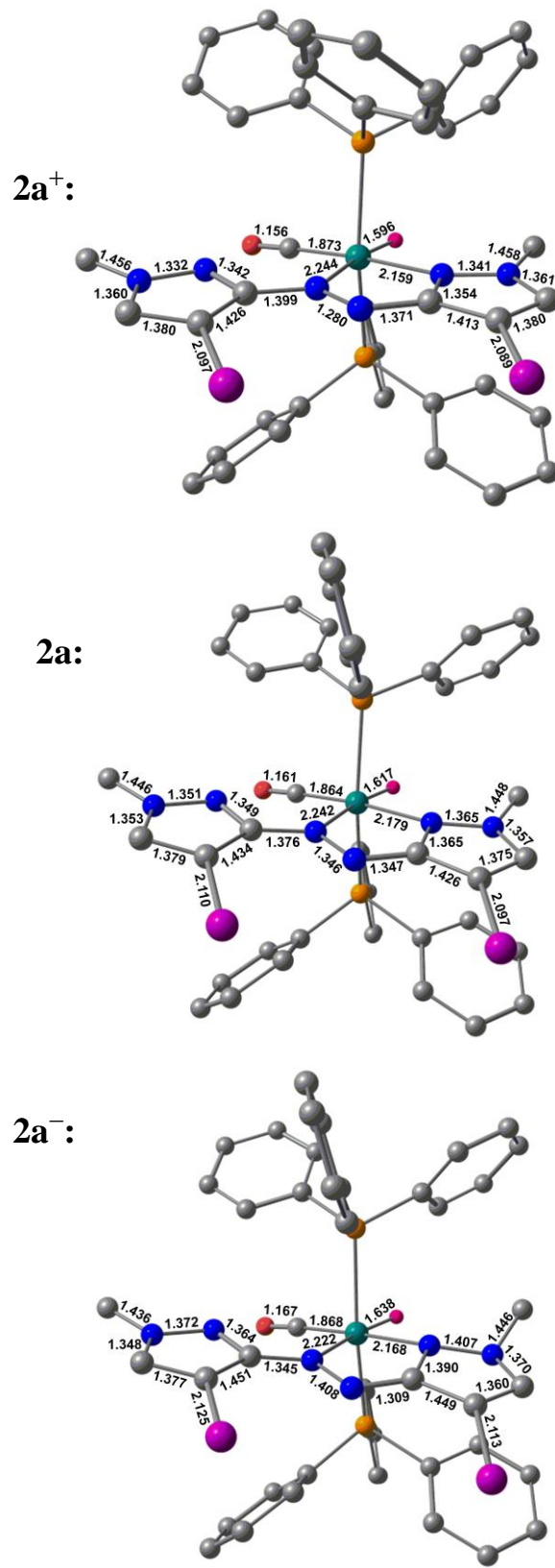


Fig. S5c DFT optimised structures of $\mathbf{2a}^n$ ($n = +1, 0, -1$).

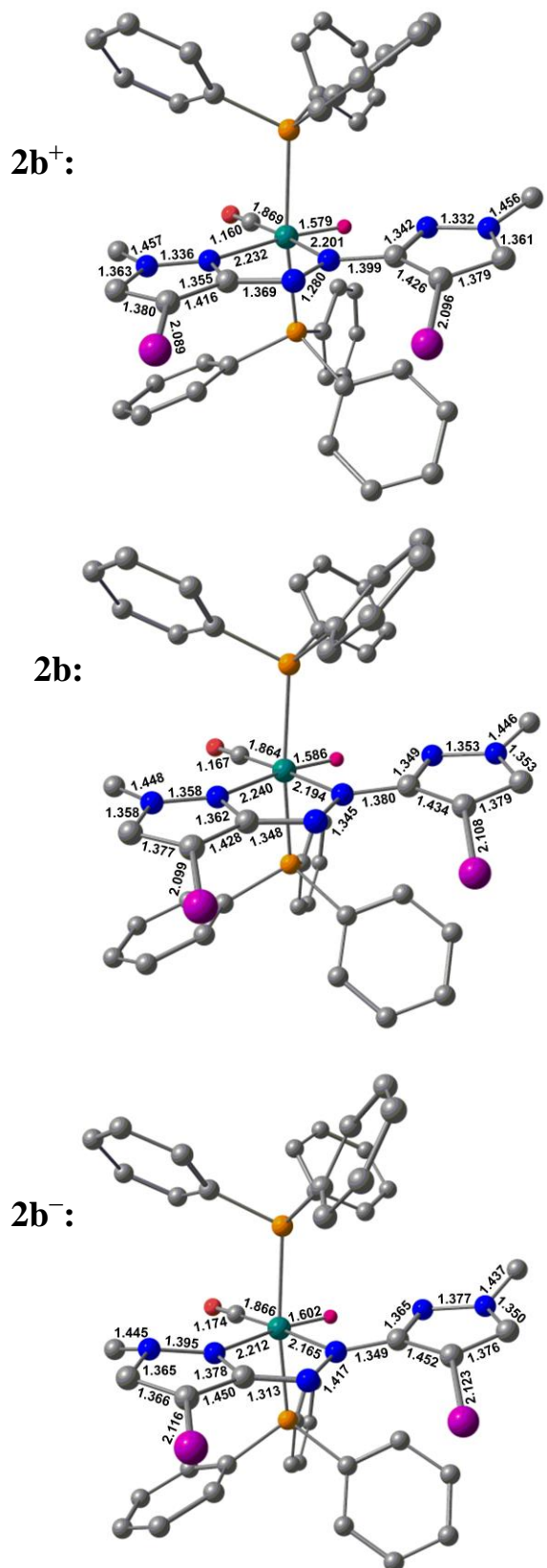


Fig. S5d DFT optimised structures of **2bⁿ** ($n = +1, 0, -1$).

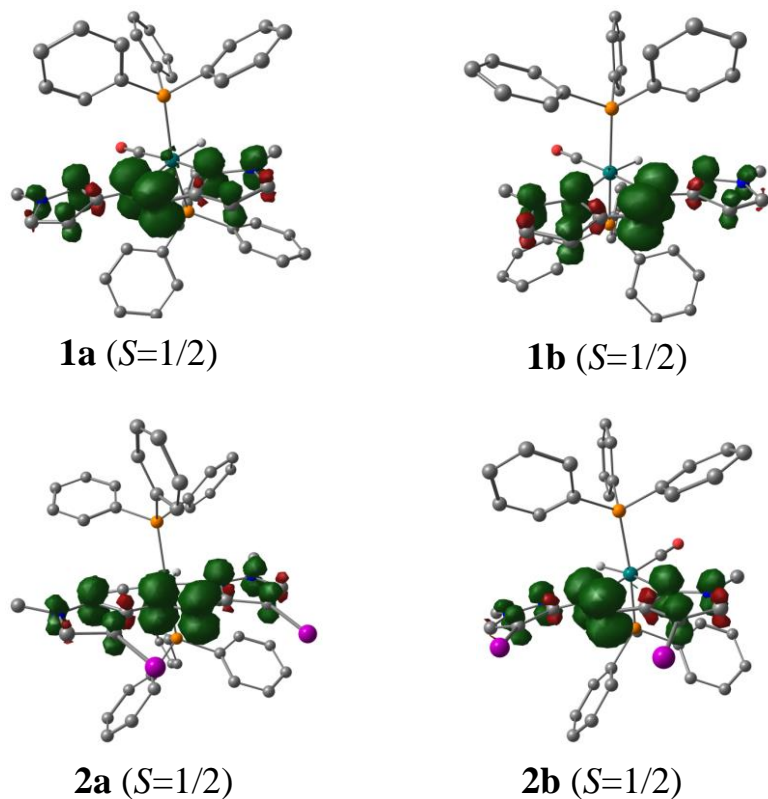


Fig. S6 DFT calculated Mulliken spin density plots for **1a**, **1b**, **2a** and **2b**.

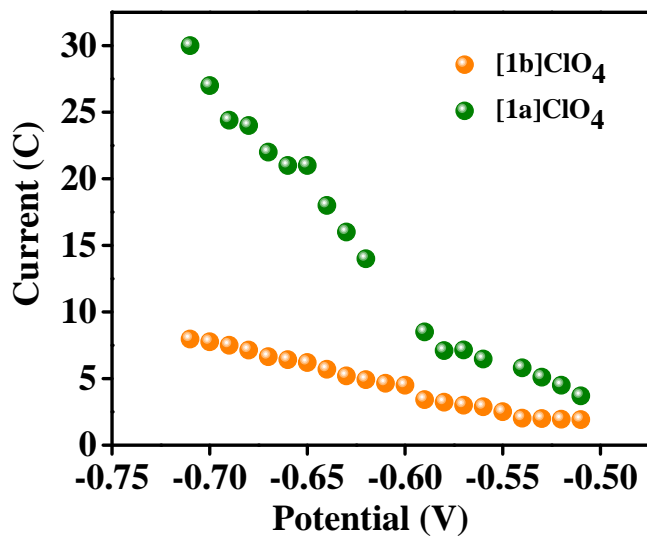


Fig. S7 Controlled-potential electrolysis of the complexes **[1a]ClO₄** and **[1b]ClO₄** in 0.5 M H₂SO₄.

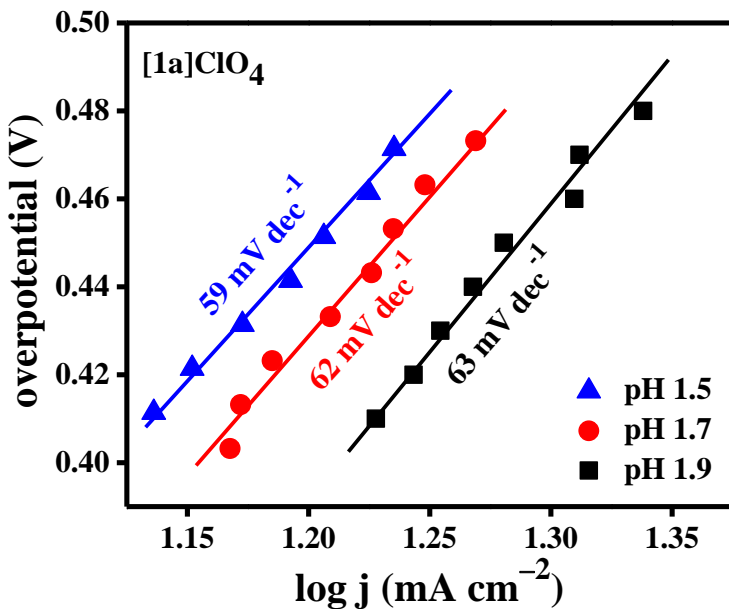


Fig. S8 Tafel slopes of the catalyst **[1a]**ClO₄ determined under controlled-potential chronoamperometric conditions at different pHs. The Tafel slope values are 59, 62 and 63 mV dec⁻¹ at pH values 1.5, 1.7, and 1.9, respectively. The Tafel slope has no significant change with variation of the pH of the solution.

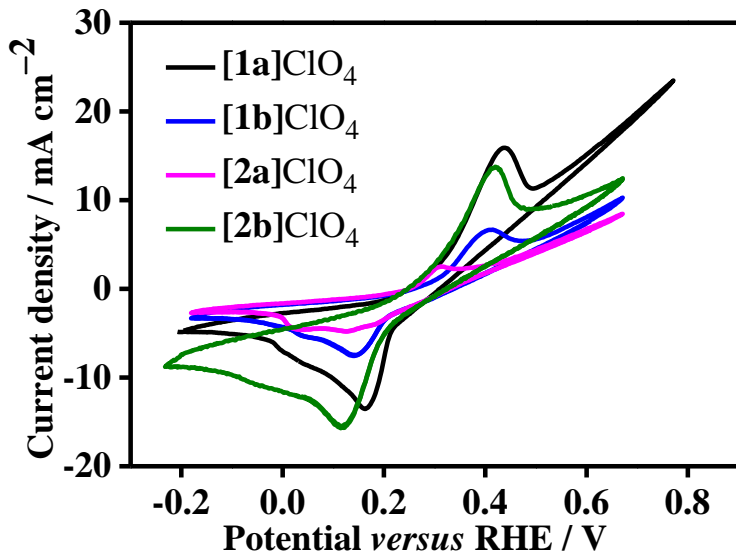


Fig. S9 Cyclic voltammetry profiles of the catalysts@CC.

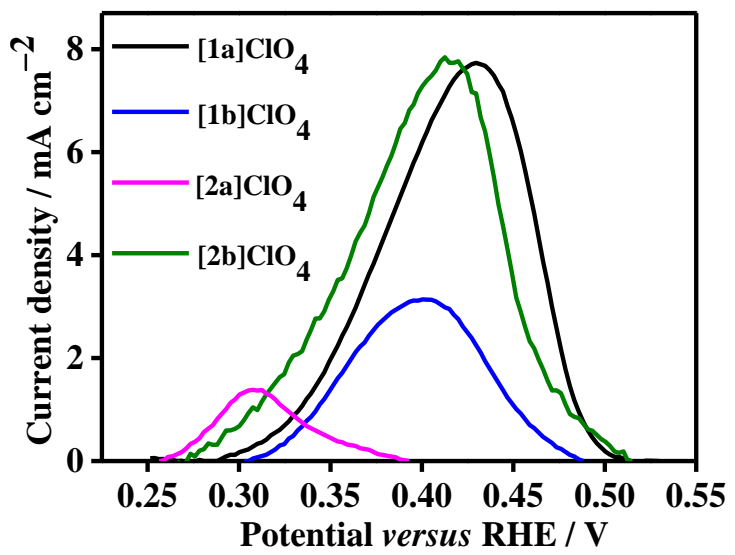


Fig. S10 Area integration of the oxidation peaks to find out the active catalytic sites of the catalysts.

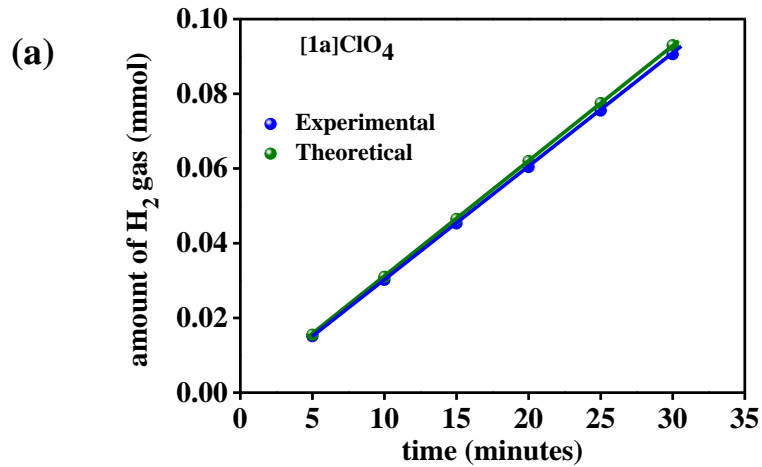


Fig. S11 (a) Faradic efficiency of **[1a]ClO₄** and (b) demonstration of the two compartment H-cell used for the Faradaic efficiency determination.

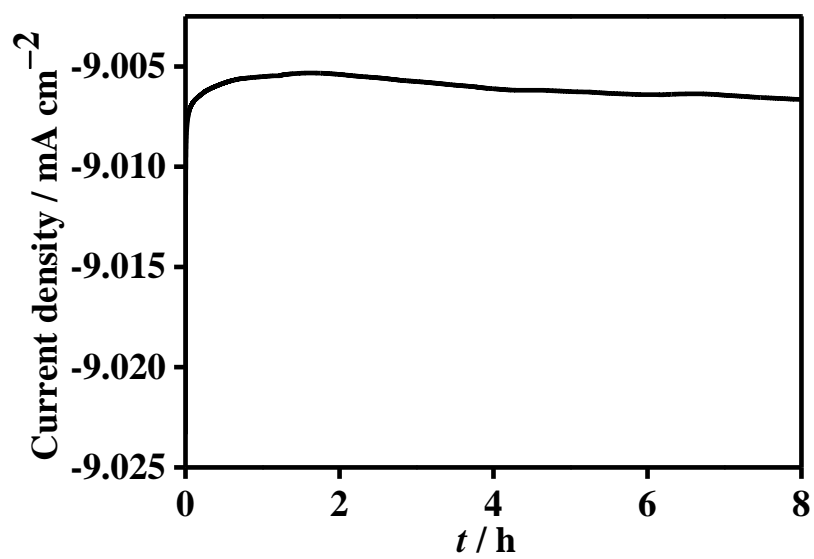


Fig. S12 Chronoamperometric stability test for the catalyst [1a]ClO₄.

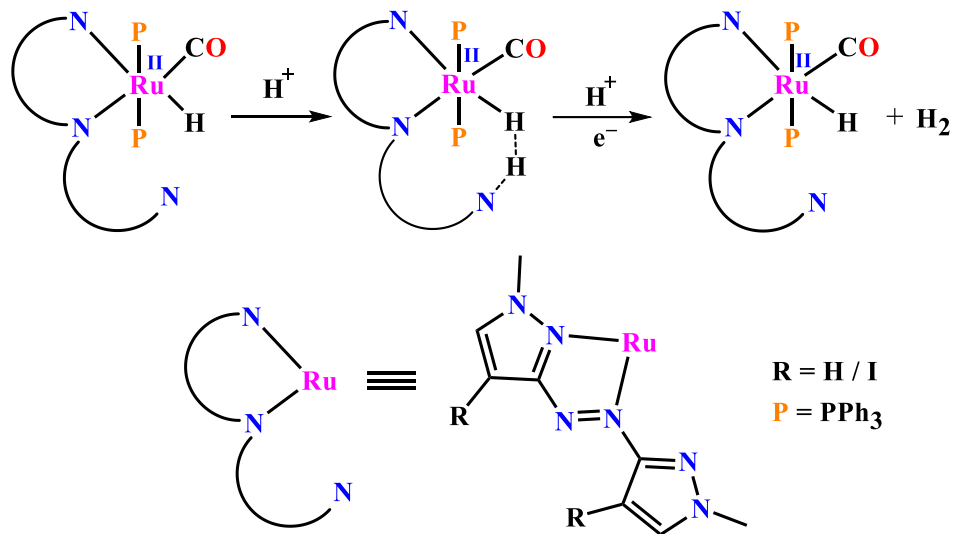


Fig. S13 PCET during the electrocatalytic HER with [1a]ClO₄.

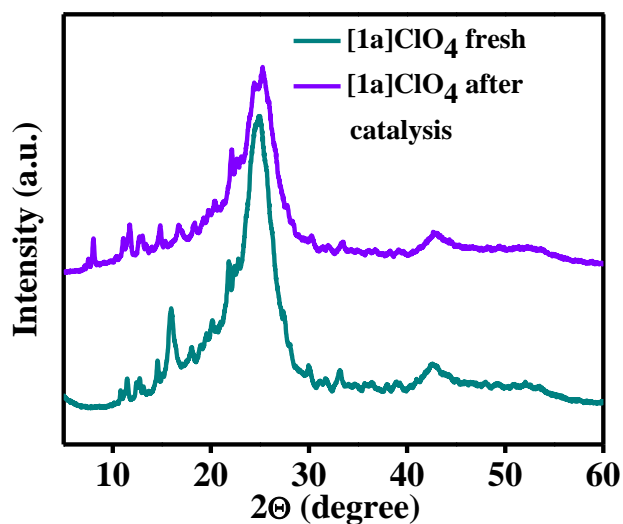


Fig. S14 PXRD of the catalyst [1a]ClO₄ after electrocatalytic HER.

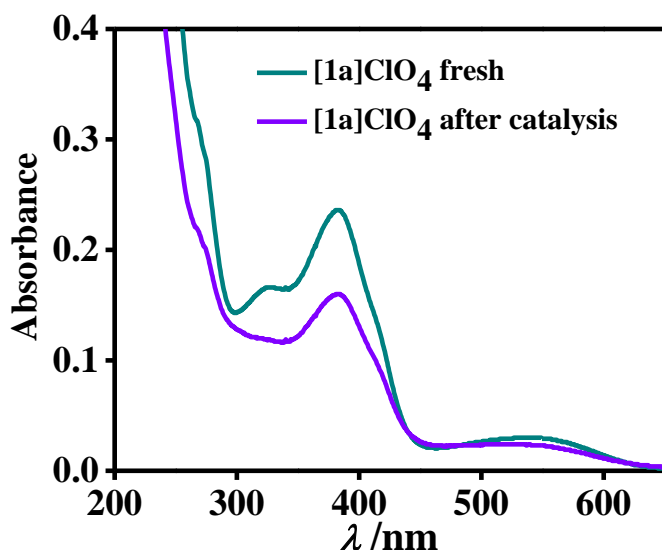


Fig. S15 UV-vis spectra of the catalyst [1a]ClO₄ after electrocatalytic HER (in acetonitrile).

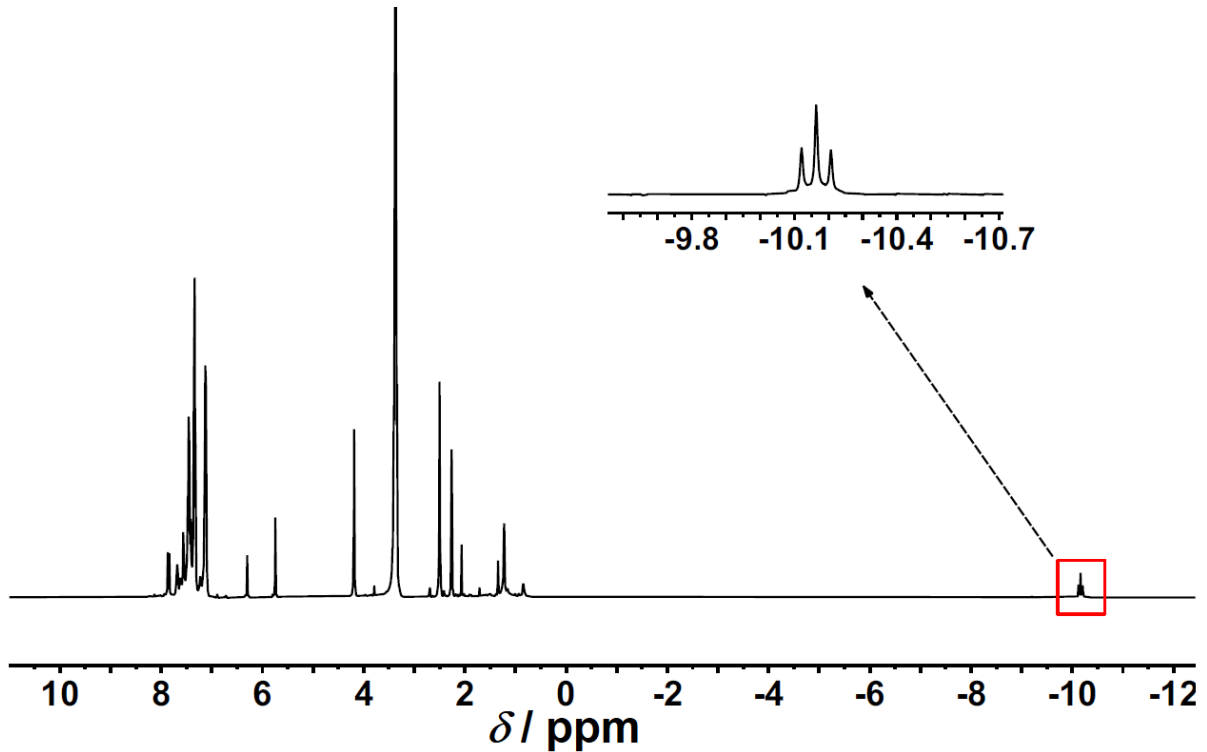


Fig. S16 ^1H -NMR spectrum of **[1a]** ClO_4 in $(\text{CD}_3)_2\text{SO}$ after electrocatalytic HER.

Equation 1 Determination of surface-active sites using area integration of the redox peaks.^{S1}

For complex [1a]ClO₄

Calculated area associated with the oxidation peak = 0.747×10^{-3} V A

Hence the associated charge is = 0.747×10^{-3} V A / 0.005 V s⁻¹ = A s = 149.4×10^{-3} C

Now, the number of electron transferred is = 149.4×10^{-3} C / 1.602×10^{-19} C = 93.25×10^{16}

Since the oxidation of Ru²⁺ to Ru³⁺ is a single electron transfer reaction, the number of electrons calculated above is the same as the number of surface-active sites. Hence, the surface-active site that participated in HER is = 93.25×10^{16} .

For complex [1b]ClO₄

Calculated area associated with the oxidation peak = 0.283×10^{-3} V A

Hence the associated charge is = 0.283×10^{-3} V A / 0.005 V s⁻¹ = 56.6×10^{-3} C

Now, the number of electron transferred is = 56×10^{-3} C / 1.602×10^{-19} C = 35.33×10^{16}

Since the oxidation of Ru²⁺ to Ru³⁺ is a single electron transfer reaction, the number of electrons calculated above is the same as the number of surface-active sites. Hence, the surface-active site that participated in HER is = 35.33×10^{16}

For complex [2a]ClO₄

Calculated area associated with the oxidation peak = 0.400×10^{-3} V A

Hence the associated charge is = 0.400×10^{-3} / 0.005 V s⁻¹ = A s = 80.0×10^{-3} C

Now, the number of electron transferred is = 80.0×10^{-3} C / 1.602×10^{-19} C = 49.94×10^{16}

Since the oxidation of Ru²⁺ to Ru³⁺ is a single electron transfer reaction, the number of electrons calculated above is the same as the number of surface-active sites. Hence, the surface-active site that participated in HER is = 49.94×10^{16}

For complex [2b]ClO₄

Calculated area associated with the oxidation peak = 0.487×10^{-3} V A

Hence the associated charge is = $0.487 \times 10^{-3} \text{ V A} / 0.005 \text{ V s}^{-1} = \text{A s} = 97.4 \times 10^{-3} \text{ C}$

Now, the number of electron transferred is = $97.4 \times 10^{-3} \text{ C} / 1.602 \times 10^{-19} \text{ C} = 60.79 \times 10^{16}$

Since the oxidation of Ru²⁺ to Ru³⁺ is a single electron transfer reaction, the number of electrons calculated above is the same as the number of surface-active sites. Hence, the surface-active site that participated in HER is = 60.79×10^{16}

Electrochemical measurement

The Tafel analysis was carried out under semi-stationary conditions recording linear sweep voltammetry (LSV) with a scan rate of 2 mV s⁻¹. The value of Tafel slope was calculated to be 32 mV dec⁻¹ for 1a-which was lower than that of the other catalysts. This value indicates the Volmer-Heyrovsky mechanism for hydrogen evolution in the acidic medium.

In addition, we have carried out the Tafel analysis under stationary conditions. Interestingly, an increase in the Tafel slope (59-63 mV dec⁻¹) was observed. Moreover, the Tafel slope is independent of the pH of the electrolyte -which indicates a similar reaction mechanism is followed in the acidic medium

The pH-dependence of current density at a constant potential has been studied and from these data the reaction order is calculated by plotting the logarithmic current density against the pH of the electrolyte. Theoretically, the reaction order against pH for a concerted proton-coupled electron transfer pathway should be zero. A minimum deviation from zero indicates better PCET process for the catalytic hydrogen evolution reaction.

Equation 1 Calculation of turn over frequency (TOF) of different catalysts^{S1}

$$\text{TOF} = (j \times N_A) / (2 \times F \times n)$$

Were,

j = current density at 399 mV

N_A = Avogadro number

F = Faraday constant

n = number of active Ru-sites

For complex [1a]ClO₄

$$\text{TOF} = [(24.73 \times 10^{-3}) (6.023 \times 10^{23})] / [(96485) (2) (93.55 \times 10^{16})]$$

$$= 8.27 \times 10^{-2} \text{ s}^{-1}$$

For complex [1b]ClO₄

$$\text{TOF} = [(7.73 \times 10^{-3}) (6.023 \times 10^{23})] / [(96485) (2) (35.33 \times 10^{16})]$$

$$= 6.83 \times 10^{-2} \text{ s}^{-1}$$

For complex [2a]ClO₄

$$\text{TOF} = [(7.94 \times 10^{-3}) (6.023 \times 10^{23})] / [(96485) (2) (49.94 \times 10^{16})]$$

$$= 4.96 \times 10^{-2} \text{ s}^{-1}$$

For complex [2b]ClO₄

$$\text{TOF} = [(7.27 \times 10^{-3}) (6.023 \times 10^{23})] / [(96485) (2) (60.79 \times 10^{16})]$$

$$= 3.73 \times 10^{-2} \text{ s}^{-1}$$

Faradic efficiency calculation

Equation 2 Calculation of the faradic efficiency of [1a]ClO₄ and [1b]ClO₄.^{S2}

To find out how much hydrogen was produced in the hydrogen evolution reaction, the water displacement method was used in a two-compartment H-type cell. The chronoamperometric test was carried out for 30 minutes at a current density of 10 mA cm⁻² to determine the amount of H₂.

First, we used the following equation derived from Faraday's law to get the theoretical amount of hydrogen.

$$n\text{H}_2 \text{ (theoretical)} = \frac{Q}{nF} = \frac{\mathbf{i} * \mathbf{t}}{\mathbf{nF}}$$

Where nH₂ denotes the theoretically calculated amount of H₂, Q is the amount of applied charge, n is the number of electrons participating in the HER reaction (2 electrons), F is the Faraday

constant ($96485.3 \text{ s A mol}^{-1}$), I is the applied current (0.01 A), and t is the reaction time (30 min).

At the time of chronoamperometric measurements, the amount of hydrogen generated during the experiment was measured and the theoretically calculated amount was compared with the actually generated amount of H_2 . Further, the faradaic efficiency was calculated using the following equation:

For 1a[ClO₄]

$$n\text{H}_2 \text{ (theoretical)} = \frac{Q}{nF} = \frac{i * t}{nF} = \frac{0.01 \text{ A} * 1800 \text{ sec}}{2 * 96485.3 \text{ mol}^{-1} \text{ sec}} = 0.093 \text{ mmole}$$

$$\text{Faradic efficiency} = \frac{\text{Experimental mmole of H}_2}{\text{Theoretical mmole of H}_2}$$

$$\text{Faradic efficiency} = \frac{0.0960 \text{ mmole}}{0.0930 \text{ mmole}} = 97.4 \%$$

Table S1a Selected crystallographic parameters

Complex	[1a]ClO ₄	[1b]ClO ₄
empirical formula	C ₄₅ H _{41.5} ClN ₆ O ₅ P ₂ Ru	C ₄₅ H ₄₁ ClN ₆ O ₅ P ₂ Ru
formula weight	944.80	944.30
crystal system	Orthorhombic	Triclinic
space group	<i>Pca2</i> ₁	<i>P-1</i>
<i>a</i> (Å)	31.1410(10)	11.7897(2)
<i>b</i> (Å)	15.7359(5)	12.8924(3)
<i>c</i> (Å)	19.1556(5)	15.6424(2)
α (deg)	90	92.2110(10)
β (deg)	90	100.2750(10)
γ (deg)	90	114.235(2)
<i>V</i> (Å ³)	9386.9(5)	2116.67(7)
<i>Z</i>	8	2
μ (mm ⁻¹)	0.508	0.563
<i>T</i> (K)	150.00(10)	150.00(10)
<i>D</i> _{calcd} (g cm ⁻³)	1.337	1.482
F(000)	3876	968
θ range(deg)	1.685 to 27.499	1.746 to 25.000
data/restraints/parameters	21461/49/1092	7441/7/546
R1, wR2 [I>2σ(I)]	0.0657, 0.1453	0.0579, 0.1501
R1, wR2(all data)	0.1382, 0.1783	0.0714, 0.1612
GOF	0.997	1.035
largest diff. peak/hole [e Å ⁻³]	1.118/-0.737	2.154/-0.941

Table S1b Selected crystallographic parameters

Complex	[2a]ClO ₄	[2b]ClO ₄
empirical formula	C ₄₅ H ₃₉ ClI ₂ N ₆ O ₅ P ₂ Ru	C ₄₅ H _{38.83} ClI ₂ N ₆ O ₅ P ₂ Ru
formula weight	1196.08	1195.91
crystal system	Monoclinic	Monoclinic
space group	<i>P</i> 12 ₁ /n1	<i>P</i> 12 ₁ /n1
<i>a</i> (Å)	11.94190(10)	17.0163(5)
<i>b</i> (Å)	20.4204(2)	16.9641(4)
<i>c</i> (Å)	18.68460(10)	17.1008(5)
α (deg)	90	90
β (deg)	93.6330(10)	111.826(3)
γ (deg)	90	90
<i>V</i> (Å ³)	4547.24(6)	4582.6(2)
<i>Z</i>	4	4
μ (mm ⁻¹)	1.884	1.870
<i>T</i> (K)	104.00(10)	150.15
<i>D</i> _{calcd} (g cm ⁻³)	1.747	1.733
F(000)	2352	2351
θ range(deg)	1.9630 to 33.1490	1.8610 to 21.9350
data/restraints/parameters	7989/1/565	8051/2/575
R1, wR2 [I>2σ(I)]	0.0369, 0.0922	0.0490, 0.1125
R1, wR2(all data)	0.0379, 0.0929	0.0502, 0.1131
GOF	1.041	1.166
largest diff. peak/hole [e Å ⁻³]	1.650/-1.536	2.162/-1.834

Table S2a Selected experimental and DFT calculated bond lengths (Å)

Bond	[1a]ClO ₄					Bond	[1b]ClO ₄	
	X-ray (molecule A)	DFT		X-ray (molecule B)	DFT		X-ray	DFT
Ru1-N2	2.104(9)	2.154	Ru2-N8	2.098(9)	2.154	Ru1-N2	2.120(4)	2.224
Ru1-N4	2.162(9)	2.237	Ru2-N10	2.135(10)	2.237	Ru1-N4	2.126(4)	2.197
Ru1-P1	2.357(3)	2.454	Ru2-P3	2.370(3)	2.454	Ru1-P1	2.3640(12)	2.457
Ru1-P2	2.365(3)	2.461	Ru2-P4	2.360(3)	2.461	Ru1-P2	2.3634(12)	2.459
Ru1-HA	1.480(6)	1.605	Ru2-H	1.84(6)	1.605	Ru1-H	1.596(18)	1.586
Ru1-C9	1.862(14)	1.878	Ru2-C54	1.846(12)	1.878	Ru1-C9	1.884(7)	1.872
N3-N4	1.304(12)	1.281	N9-N10	1.298(12)	1.281	N3-N4	1.279(6)	1.280
N1-N2	1.320(12)	1.340	N7-N8	1.327(12)	1.340	N1-N2	1.340(6)	1.337
N5-N6	1.369(15)	1.337	N7-C46	1.482(14)	1.458	N5-N6	1.323(8)	1.336
N1-C1	1.440(14)	1.458	N7-C47	1.377(13)	1.362	N1-C1	1.439(8)	1.457
N1-C2	1.369(14)	1.362	C54-O6	1.169(12)	1.155	N1-C2	1.361(8)	1.365
N2-C4	1.391(15)	1.355	-	-	-	N2-C4	1.353(7)	1.352
N3-C4	1.399(17)	1.372	-	-	-	N3-C4	1.367(7)	1.372
N4-C5	1.407(15)	1.401	-	-	-	N4-C5	1.423(7)	1.402
N5-C5	1.342(17)	1.340	-	-	-	N5-C5	1.350(9)	1.340
C9-O1	1.105(13)	1.155	-	-	-	C9-O1	1.184(7)	1.159
C3-I1	-	-	-	-	-	C3-I1	-	-
C6-I2	-	-	-	-	-	C6-I2	-	-

Table S2b Selected experimental and DFT calculated bond lengths (Å)

Bond	[2a]ClO ₄		[2b]ClO ₄	
	X-ray	DFT	X-ray	DFT
Ru1-N2	2.116(3)	2.159	2.178(5)	2.232
Ru1-N4	2.149(3)	2.244	2.129(5)	2.201
Ru1-P1	2.3844(10)	2.453	2.3705(13)	2.461
Ru1-P2	2.3633(10)	2.467	2.3580(13)	2.449
Ru1-H	1.51(2)	1.596	1.49(2)	1.579
Ru1-C9	1.839(4)	1.873	1.835(6)	1.869
N3-N4	1.296(5)	1.280	1.298(6)	1.280
N1-N2	1.342(5)	1.341	1.333(6)	1.336
N5-N6	1.336(5)	1.332	1.326(6)	1.332
N1-C1	1.460(5)	1.458	1.439(8)	1.457
N1-C2	1.370(5)	1.361	1.375(8)	1.363
N2-C4	1.343(5)	1.354	1.339(7)	1.355
N3-C4	1.379(5)	1.371	1.369(7)	1.369
N4-C5	1.396(5)	1.399	1.391(7)	1.399
N5-C5	1.339(5)	1.342	1.326(7)	1.342
C9-O1	1.159(5)	1.156	1.158(7)	1.160
C3-I1	2.040(4)	2.089	2.096(6)	2.089
C6-I2	2.057(4)	2.097	2.060(6)	2.096

Table S3a Selected experimental and DFT calculated bond angles (deg)

Bond angles	[1a]ClO ₄					Bond angles	[1b]ClO ₄	
	X-ray (molecule A)	DFT	X-ray (molecule B)	X- ray	DFT		X-ray	DFT
N2-Ru1-N4	73.3(4)	72.2	N8-Ru2-N10	72.9(4)	72.2	N2-Ru1-N4	72.80(16)	72.4
N2-Ru1-P1	90.7(2)	91.9	N8-Ru2-P3	92.2(2)	91.9	N2-Ru1-P1	95.18(11)	94.9
N2-Ru1-P2	92.3(2)	91.4	N8-Ru2-P4	92.1(2)	91.4	N2-Ru1-P2	95.33(11)	94.3
N2-Ru1-C9	175.8(5)	173.8	N8-Ru2-C54	174.5(4)	173.8	N2-Ru1-C9	96.4(2)	101.3
N2-Ru1-HA	96.0(2)	96.1	N8-Ru2-H	92.4(19)	96.1	N2-Ru1-H	161.7(12)	167.0
N4-Ru1-P1	100.7(2)	98.7	N10-Ru2-P3	100.8(2)	98.7	N4-Ru1-P1	93.72(11)	93.2
N4-Ru1-P2	94.2(2)	98.6	N10-Ru2-P4	94.9(2)	98.6	N4-Ru1-P2	90.70(11)	93.7
N4-Ru1-C9	102.7(5)	101.5	N10-Ru2-C54	101.6(4)	101.5	N4-Ru1-C9	169.0(2)	173.8
N4-Ru1-HA	167(2)	168.3	N10-Ru2-H	165(2)	168.3	N4-Ru1-H	89.0(12)	94.5
P1-Ru1-P2	165.04(10)	162.5	-	-	-	P1-Ru1-P2	169.40(5)	169.6
P1-Ru1-C9	88.6(3)	89.0	-	-	-	P1-Ru1-C9	89.06(18)	86.8
P1-Ru1-HA	86(2)	81.5	-	-	-	P1-Ru1-H	84.1(13)	85.8
P2-Ru1-C9	89.5(3)	89.4	-	-	-	P2-Ru1-C9	88.41(18)	87.0
P2-Ru1-HA	79(2)	81.0	-	-	-	P2-Ru1-H	86.4(13)	86.0
C9-Ru1-HA	88(3)	90.0	-	-	-	C9-Ru1-H	101.9(12)	91.5

Table S3b Selected experimental and DFT calculated bond angles (deg)

Bond angles	[2a]ClO ₄		[2b]ClO ₄	
	X-ray	DFT	X-ray	DFT
N2-Ru1-N4	73.14(13)	71.8	73.31(17)	72.1
N2-Ru1-P1	89.69(9)	91.7	97.52(12)	97.2
N2-Ru1-P2	93.04(9)	90.4	96.90(12)	94.2
N2-Ru1-C9	177.36(16)	174.3	99.9(2)	103.4
N2-Ru1-H	99(2)	96.7	162(5)	166.3
N4-Ru1-P1	92.80(9)	97.0	91.46(12)	92.5
N4-Ru1-P2	90.90(9)	95.5	91.46(12)	93.0
N4-Ru1-C9	104.63(15)	102.9	173.2(2)	175.4
N4-Ru1-H	172(3)	168.6	88(5)	94.3
P1-Ru1-P2	175.92(4)	167.2	165.54(5)	168.2
P1-Ru1-C9	91.83(12)	86.5	89.72(16)	88.5
P1-Ru1-H	91(3)	82.7	83(5)	84.8
P2-Ru1-C9	85.56(12)	92.3	88.87(16)	86.7
P2-Ru1-H	86(3)	84.5	83(5)	84.4
C9-Ru1-H	83(2)	88.4	98(5)	90.1

Table S4 Experimental and TD-DFT (M06L/CPCM/CH₃CN) calculated electronic transitions for **1ⁿ** and **2ⁿ** (*n* = +1, 0) in CH₃CN.

$\lambda_{\text{max}}^{\text{a}}/\text{nm}$ (expt.) (ϵ/dm^3 $\text{mol}^{-1}\text{cm}^{-1}$) ^b	$\lambda^{\text{c}}/\text{nm}$ (DFT) (<i>f</i>)	Transitions	Character
1a⁺ (S = 0)			
496(459)	2140(0.057)	HOMO→LUMO(0.68)	PPh ₃ (π)/Ru(d π)→L1(π^*)
432(428)	3400(0.050)	HOMO-1→LUMO(0.59)	L1(π)/Ru(d π)→L1(π^*)
366(359)	8380(0.262)	HOMO-3→LUMO(0.48) HOMO-1→LUMO(0.34)	PPh ₃ (π)→L1(π^*) L1(π)/Ru(d π)→L1(π^*)
274(264)	10580(0.231)	HOMO-3→LUMO+1(0.35)	PPh ₃ (π)→PPh ₃ (π^*)/Ru(d π)
1a (S = 1/2)			
320(314)	7220(0.067)	HOMO-2(α)→LUMO(α)(0.57)	Ru(d π)/PPh ₃ (π)→PPh ₃ (π^*)/Ru(d π)
234(244)	28740(0.014)	HOMO(α)→LUMO-15(α)(0.32)	L1(π)→PPh ₃ (π^*)/Ru(d π)
1b⁺ (S = 0)			
540(520)	1520(0.037)	HOMO→LUMO(0.68)	Ru(d π)/PPh ₃ (π)→L1(π^*)
382(374)	11420(0.264)	HOMO-2→LUMO(0.50)	PPh ₃ (π)→L1(π^*)
321(337)	8120(0.094)	HOMO→LUMO+1(0.60)	Ru(d π)/PPh ₃ (π)→PPh ₃ (π^*)/Ru(d π)
233(260)	26240(0.210)	HOMO-2→LUMO+1(0.57)	PPh ₃ (π)→PPh ₃ (π^*)/Ru(d π)
1b (S = 1/2)			
500(460)	2000(0.069)	HOMO(β)→LUMO(β)(0.32)	L1(π)→L1(π^*)
378(389)	14160(0.069)	HOMO-1(β)→LUMO(β)(0.81)	Ru(d π)/L1(π)→L1(π^*)
234(255)	30800(0.175)	HOMO-4(β)→LUMO+1(β)(0.50)	L1(π)/Ru(d π)→PPh ₃ (π^*)/Ru(d π)
2a⁺ (S = 0)			
507(492)	3560(0.059)	HOMO→LUMO(0.68)	PPh ₃ (π)/Ru(d π)→L2(π^*)
385(406)	6740(0.166)	HOMO-2→LUMO(0.54)	Ru(d π)/L2(π)→L2(π^*)
278(300)	11100(0.120)	HOMO-1→LUMO+1(0.37) HOMO-2→LUMO+1(0.32)	L2(π)/Ru(d π)→PPh ₃ (π^*)/Ru(d π) Ru(d π)/L2(π)→PPh ₃ (π^*)/Ru(d π)
2a (S = 1/2)			
380(377)	10560(0.076)	HOMO-1(β)→LUMO(β)(0.78)	L2(π)/Ru(d π)→L2(π^*)
256(261)	26020(0.153)	HOMO-4(α)→LUMO+1(α)(0.20)	Ru(d π)→PPh ₃ (π^*)/Ru(d π)
2b⁺ (S = 0)			
511(548)	12760(0.049)	HOMO→LUMO(0.68)	PPh ₃ (π)/Ru(d π)→L2(π^*)
457(442)	19240(0.054)	HOMO-1→LUMO(0.56)	L2(π)/PPh ₃ (π)→L2(π^*)
397(393)	15280(0.108)	HOMO-3→LUMO(0.60)	L2(π)/PPh ₃ (π)→L2(π^*)
230(230)	24040(0.029)	HOMO-2→LUMO+6(0.25)	PPh ₃ (π)/Ru(d π)→PPh ₃ (π^*)/L2(π^*)
2b (S = 1/2)			
367(363)	9420(0.012)	HOMO-2(β)→LUMO(β)(0.12)	L2(π)→L2(π^*)/PPh ₃ (π^*)
242(252)	30480(0.019)	HOMO-4(β)→LUMO+2(β)(0.12)	PPh ₃ (π)/Ru(d π)→PPh ₃ (π^*)

^a Experimental absorption maximum in CH₃CN. ^b Molar Extinction coefficients in dm³ mol⁻¹ cm⁻¹. ^c Calculated oscillator strength.

Table S5 Energies of DFT (M06L/lanL2DZ/6-31G**) optimised structures

Complex	E (Hartrees)				$E_{(\text{HE-LE})}^a$
		$S = 0$	$S = 1/2$	$S = 1$	
1a⁺	-2919.6889	-	-	-	-
1a	-	-2919.8370	-	-	-
1a⁻	-2919.8421	-	-2919.8331	0.009 Hartrees 23.63 KJ mol ⁻¹ 1975.27 cm ⁻¹	
1b⁺	-2919.6794	-	-	-	-
1b	-	-2919.8308	-	-	-
1b⁻	-2919.8367		-2919.8264	0.0103 Hartrees 27.04 KJ mol ⁻¹ 2260.58 cm ⁻¹	
2a⁺	-2941.2188	-	-	-	-
2a	-	-2941.3745	-	-	-
2a⁻	-2941.3949	-	-2941.3760	0.0189 Hartrees 49.62 KJ mol ⁻¹ 4148.07 cm ⁻¹	
2b⁺	-2941.2173	-	-	-	-
2b		-2941.3751		-	
2b⁻	-2941.3949		-2941.3753	0.0196 Hartrees 51.45 KJ mol ⁻¹ 4301.70 cm ⁻¹	

^aHE = Spin state in higher in energy and LE = Spin state in lower in energy

Table S6 Composition and energies of selected molecular orbitals of **1a⁺** (*S*=0)

MO	Energy(eV)	% Composition				
		Ru	L1	PPh ₃	CO	H
HOMO-5	-9.003	39	20	29	08	05
HOMO-4	-8.983	10	03	86	00	00
HOMO-3	-8.880	06	04	90	00	00
HOMO-2	-8.786	01	01	98	00	00
HOMO-1	-8.703	28	53	17	02	00
HOMO	-8.298	22	11	67	00	00
LUMO	-5.133	11	78	10	00	00
LUMO-1	-3.353	30	04	65	02	01
LUMO-2	-2.899	08	09	81	01	00
LUMO-3	-2.860	12	08	75	05	01
LUMO-4	-2.807	03	04	91	02	01
LUMO-5	-2.750	08	06	83	02	02

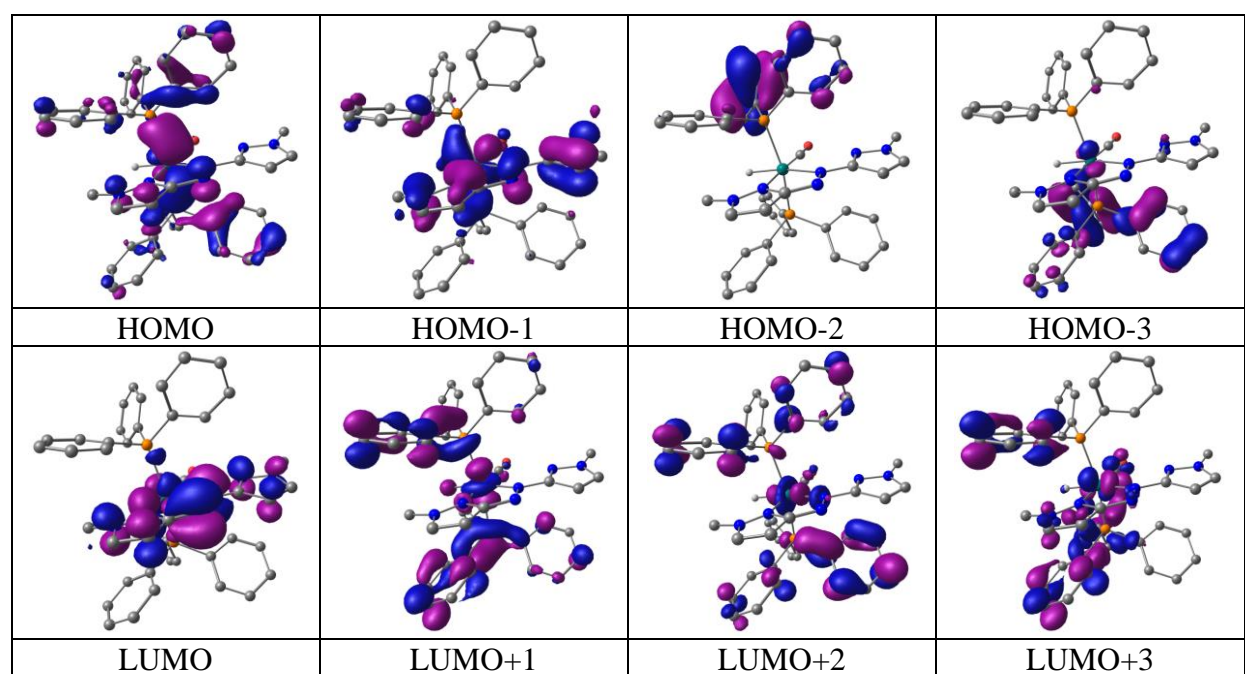


Table S7 Composition and energies of selected molecular orbitals of **1a** ($S = 1/2$)

MO	Energy(eV)	% Composition				
		Ru	L1	PPh ₃	CO	H
α -spin						
HOMO-5	-5.964	55	34	03	05	03
HOMO-4	-5.850	54	29	11	05	00
HOMO-3	-5.638	34	51	04	07	05
HOMO-2	-5.518	50	19	31	00	00
HOMO-1	-5.252	19	75	04	01	00
SOMO	-3.034	08	85	06	00	00
LUMO	-0.726	24	04	71	01	00
LUMO+1	-0.515	02	02	95	00	01
LUMO+2	-0.442	04	00	95	00	00
LUMO+3	-0.397	07	01	92	01	00
LUMO+4	-0.377	05	04	91	00	00
LUMO+5	-0.209	04	02	93	01	00
β -spin						
HOMO-5	-5.899	69	19	02	08	01
HOMO-4	-5.884	02	94	04	00	00
HOMO-3	-5.767	58	27	09	06	00
HOMO-2	-5.493	20	66	04	05	06
HOMO-1	-5.385	55	17	28	00	00
HOMO	-4.783	11	86	03	01	00
LUMO	-0.970	10	78	71	01	00
LUMO+1	-0.719	23	04	78	01	00
LUMO+2	-0.514	02	02	95	00	00
LUMO+3	-0.438	03	01	96	00	00
LUMO+4	-0.393	06	01	92	01	00
LUMO+5	-0.370	05	03	91	00	00

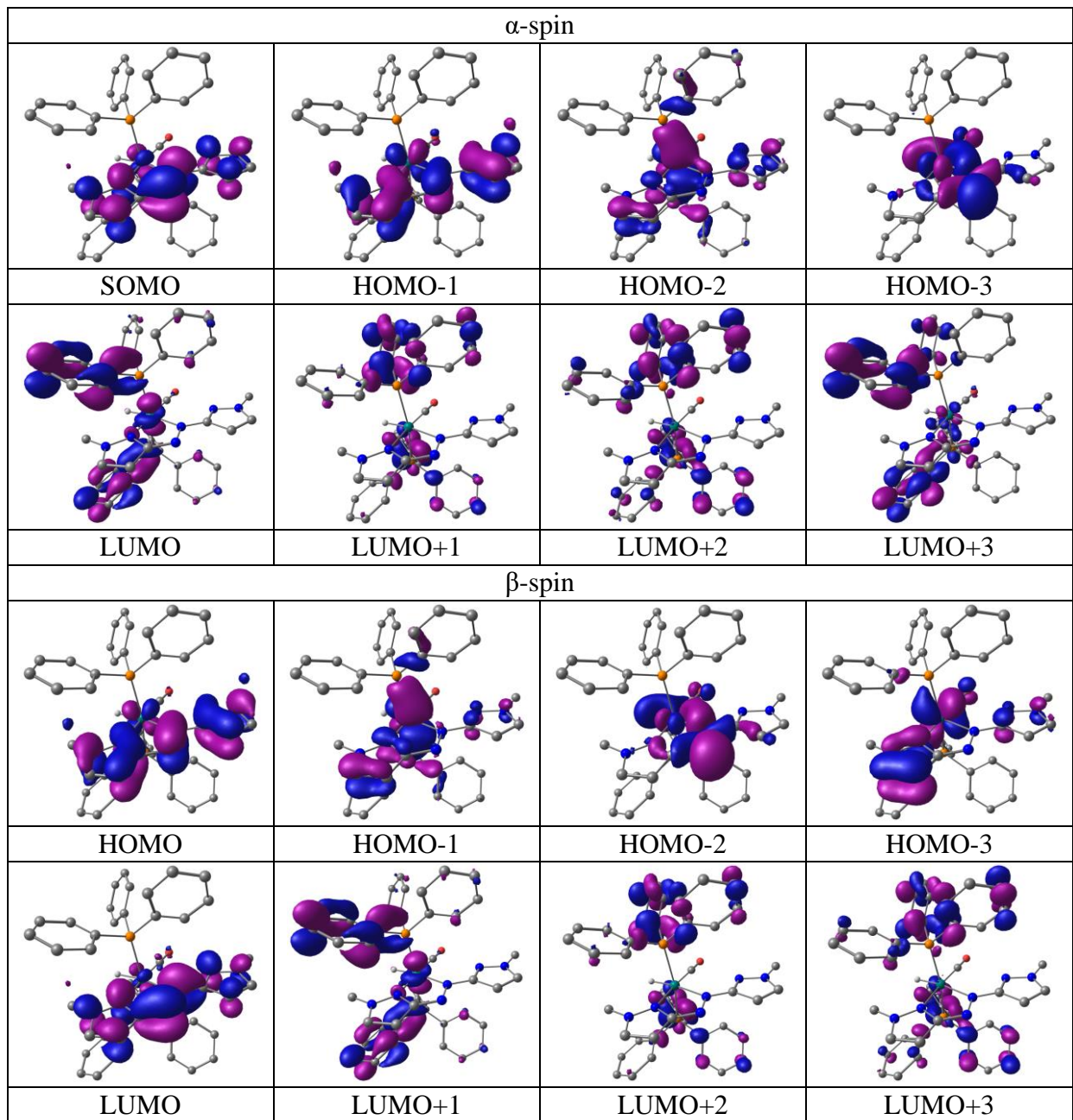


Table S8 Composition and Energies of Selected Molecular Orbitals of **1a⁻** (*S* = 0)

MO	Energy(eV)	% Composition				
		Ru	L1	PPh ₃	CO	H
HOMO-5	-2.690	52	33	09	06	00
HOMO-4	-2.663	74	12	03	11	00
HOMO-3	-2.191	43	22	35	01	00
HOMO-2	-1.920	12	75	05	02	06
HOMO-1	-1.606	18	72	08	01	01
HOMO	1.469	16	60	23	01	00
LUMO	1.990	10	01	88	00	00
LUMO+1	2.048	17	02	80	01	00
LUMO+2	2.272	04	06	89	00	00
LUMO+3	2.280	04	02	93	01	00
LUMO+4	2.330	05	03	92	00	00
LUMO+5	2.471	06	02	91	01	00

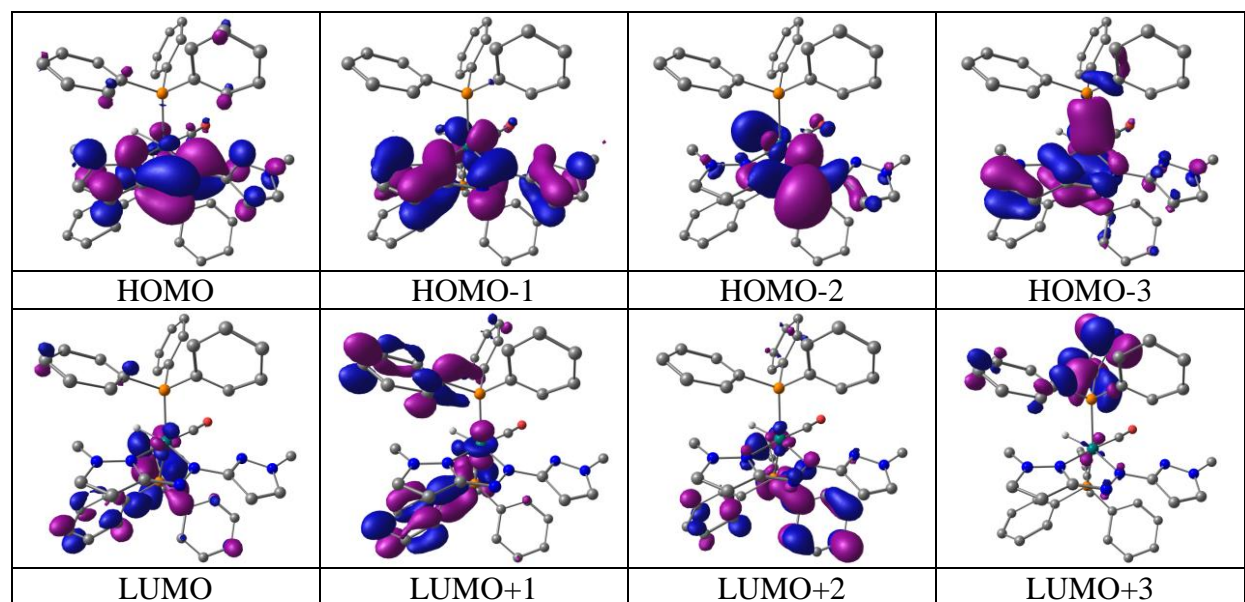


Table S9 Composition and energies of selected molecular orbitals of **1b⁺** ($S = 0$)

MO	Energy(eV)	% Composition				
		Ru	L1	PPh ₃	CO	H
HOMO-5	-8.949	39	02	54	05	00
HOMO-4	-8.911	18	20	62	00	00
HOMO-3	-8.852	02	34	64	00	00
HOMO-2	-8.778	01	01	97	00	06
HOMO-1	-8.570	24	21	55	00	01
HOMO	-8.185	50	11	38	00	00
LUMO	-5.125	07	85	06	01	00
LUMO+1	-3.346	33	03	61	03	00
LUMO+2	-3.005	11	09	76	03	01
LUMO+3	-2.875	05	01	91	03	00
LUMO+4	-2.837	02	03	94	00	00
LUMO+5	-2.773	02	00	97	01	00

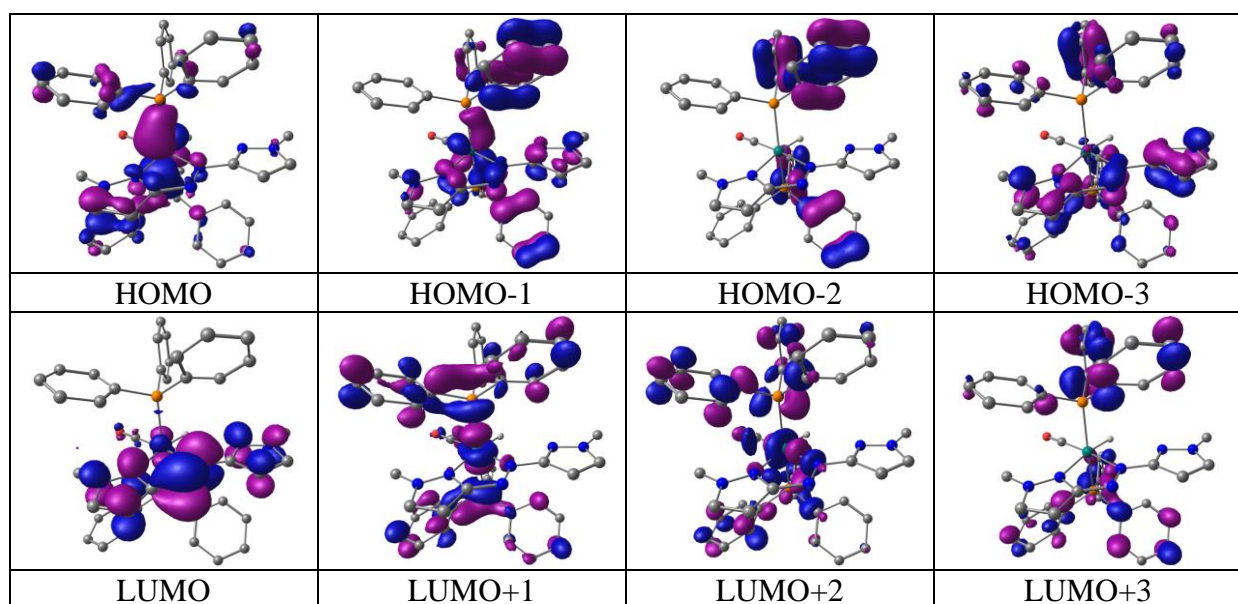


Table S10 Composition and energies of selected molecular orbitals of **1b** ($S = 1/2$)

MO	Energy(eV)	% Composition				
		Ru	L1	PPh ₃	CO	H
α -spin						
HOMO-5	-6.072	09	78	09	04	00
HOMO-4	-6.034	36	18	43	03	00
HOMO-3	-5.883	80	03	03	14	00
HOMO-2	-5.470	32	51	17	00	00
HOMO-1	-5.192	39	52	08	01	00
SOMO	-3.104	07	86	06	01	00
LUMO	-0.720	23	03	72	02	00
LUMO+1	-0.537	06	01	92	00	00
LUMO+2	-0.531	04	01	95	01	00
LUMO+3	-0.419	06	06	87	01	00
LUMO+4	-0.338	04	00	95	00	00
LUMO+5	-0.192	03	00	95	02	00
β -spin						
HOMO-5	-6.024	42	09	46	03	00
HOMO-4	-5.889	20	71	05	04	00
HOMO-3	-5.875	62	23	03	11	00
HOMO-2	-5.845	14	76	03	07	00
HOMO-1	-5.268	59	22	19	00	00
HOMO	-4.805	09	87	03	01	00
LUMO	-1.011	09	79	10	03	00
LUMO+1	-0.715	22	03	73	02	00
LUMO+2	-0.535	06	01	92	00	00
LUMO+3	-0.527	04	01	95	00	00
LUMO+4	-0.412	06	06	87	01	00
LUMO+5	-0.334	04	01	95	01	00

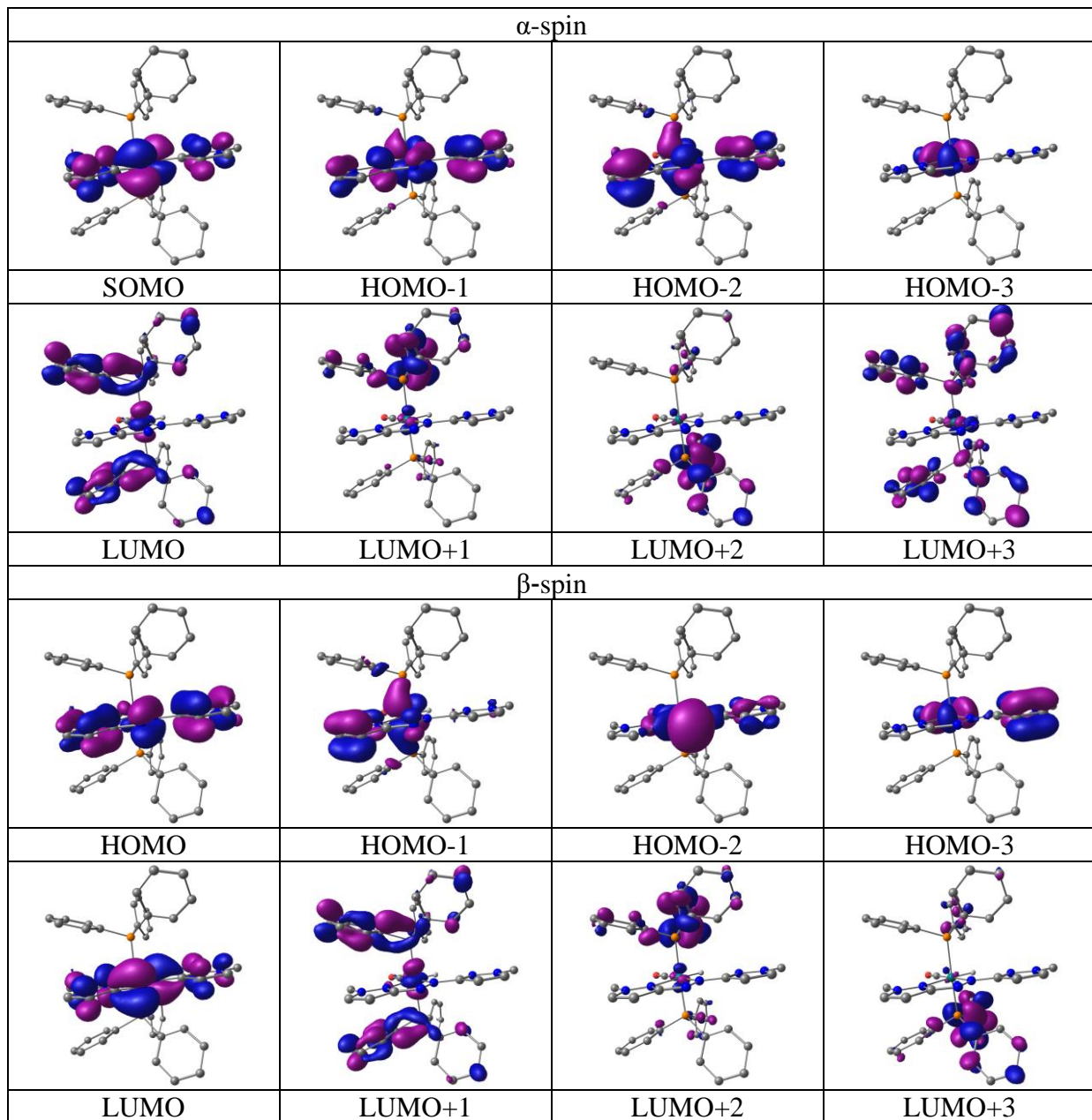


Table S11 Composition and energies of selected molecular orbitals of **1b⁻** ($S = 0$)

MO	Energy(eV)	% Composition				
		Ru	L1	PPh ₃	CO	H
HOMO-5	-2.835	78	05	02	14	00
HOMO-4	-2.727	01	92	07	00	00
HOMO-3	-2.302	21	68	05	05	00
HOMO-2	-2.259	42	46	10	01	00
HOMO-1	-1.417	06	89	04	01	00
HOMO	0.690	09	78	11	02	00
LUMO	1.760	04	02	94	01	00
LUMO+1	1.796	03	00	96	00	00
LUMO+2	1.906	18	03	78	01	00
LUMO+3	2.040	07	03	89	01	00
LUMO+4	2.114	03	01	96	01	00
LUMO+5	2.235	02	01	97	00	00

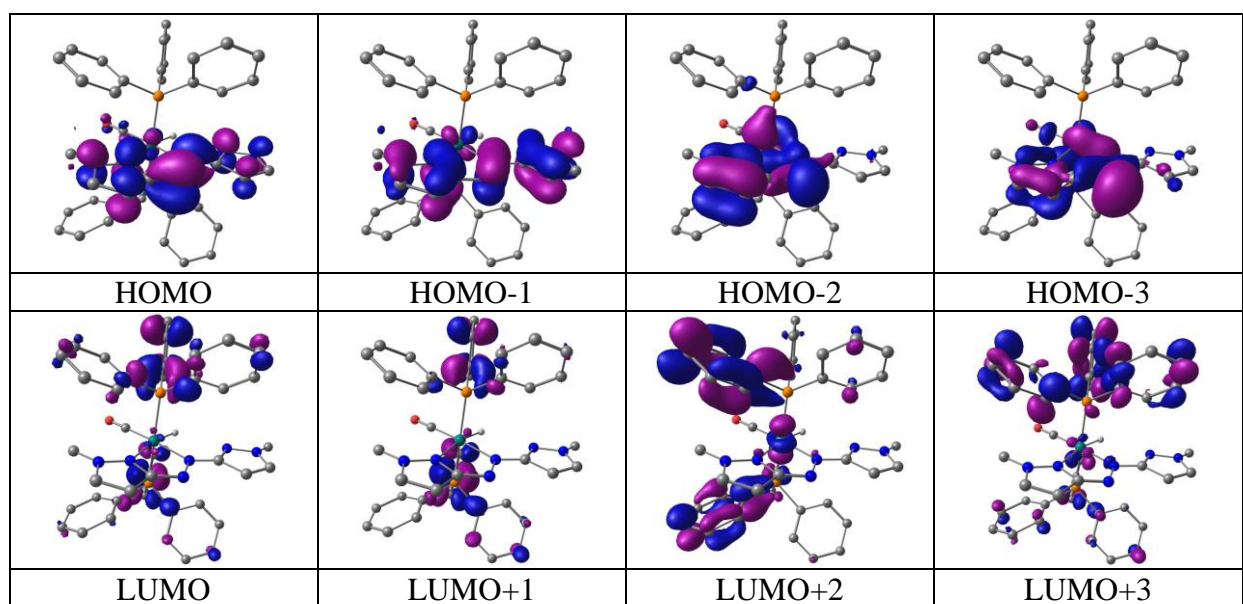


Table S12 Composition and energies of selected molecular orbitals of **2a⁺** ($S = 0$)

MO	Energy(eV)	% Composition				
		Ru	L2	PPh ₃	CO	H
HOMO-5	-8.895	24	34	37	04	00
HOMO-4	-8.865	18	27	52	03	01
HOMO-3	-8.831	35	38	21	05	01
HOMO-2	-8.739	38	32	30	01	00
HOMO-1	-8.616	19	67	12	01	00
HOMO	-8.261	34	11	55	00	00
LUMO	-5.139	07	85	07	00	00
LUMO+1	-3.429	29	12	56	02	01
LUMO+2	-3.255	04	86	09	01	00
LUMO+3	-2.992	00	95	04	00	00
LUMO+4	-2.958	02	30	67	01	00
LUMO+5	-2.893	04	03	92	01	00

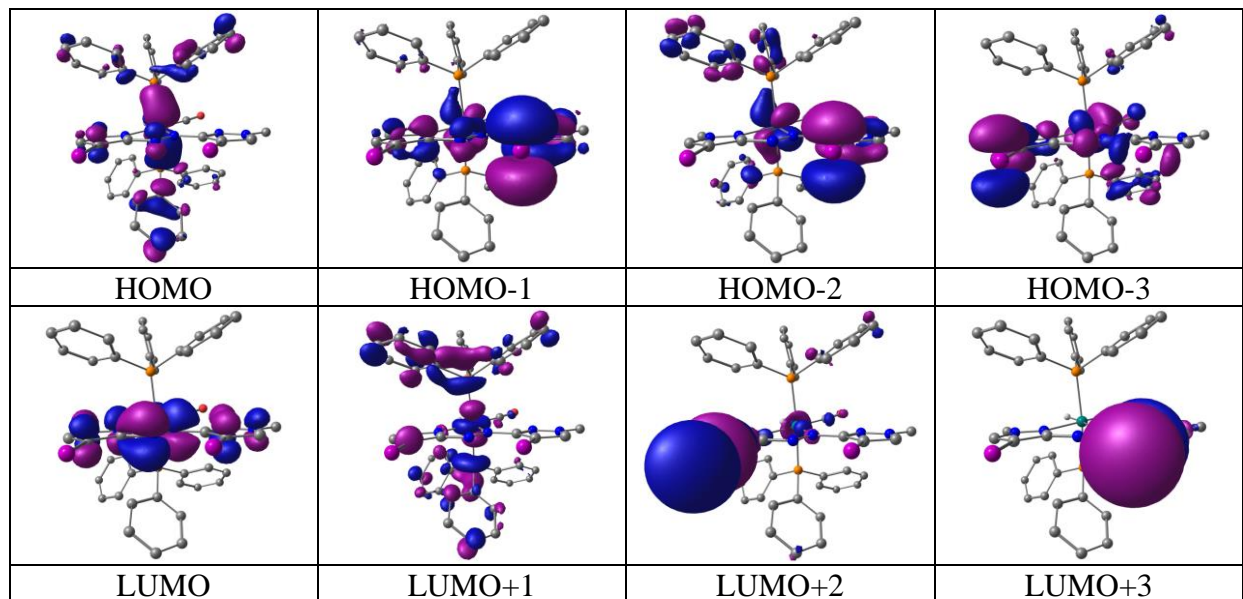


Table S13 Composition and energies of selected molecular orbitals of **2a** ($S = 1/2$)

MO	Energy(eV)	% Composition				
		Ru	L2	PPh ₃	CO	H
α -spin						
HOMO-5	-5.967	16	71	11	01	00
HOMO-4	-5.831	49	38	09	05	00
HOMO-3	-5.687	26	59	10	03	03
HOMO-2	-5.650	22	58	18	01	01
HOMO-1	-5.409	22	70	07	01	00
SOMO	-3.351	07	85	07	00	00
LUMO	-0.859	23	06	69	02	01
LUMO+1	-0.645	05	04	91	01	00
LUMO+2	-0.494	09	02	88	00	00
LUMO+3	-0.415	03	01	94	01	00
LUMO+4	-0.394	05	33	61	00	00
LUMO+5	-0.321	09	04	87	00	00
β -spin						
HOMO-5	-5.970	76	12	02	10	00
HOMO-4	-5.770	43	48	06	03	00
HOMO-3	-5.741	14	78	07	02	00
HOMO-2	-5.555	37	43	18	01	01
HOMO-1	-5.522	15	71	10	02	02
HOMO	-5.040	14	81	05	00	00
LUMO	-1.314	08	80	11	01	00
LUMO+1	-0.849	22	06	70	02	01
LUMO+2	-0.641	05	03	91	01	00
LUMO+3	-0.491	10	02	88	00	00
LUMO+4	-0.411	03	01	95	01	00
LUMO+5	-0.384	05	23	70	00	00

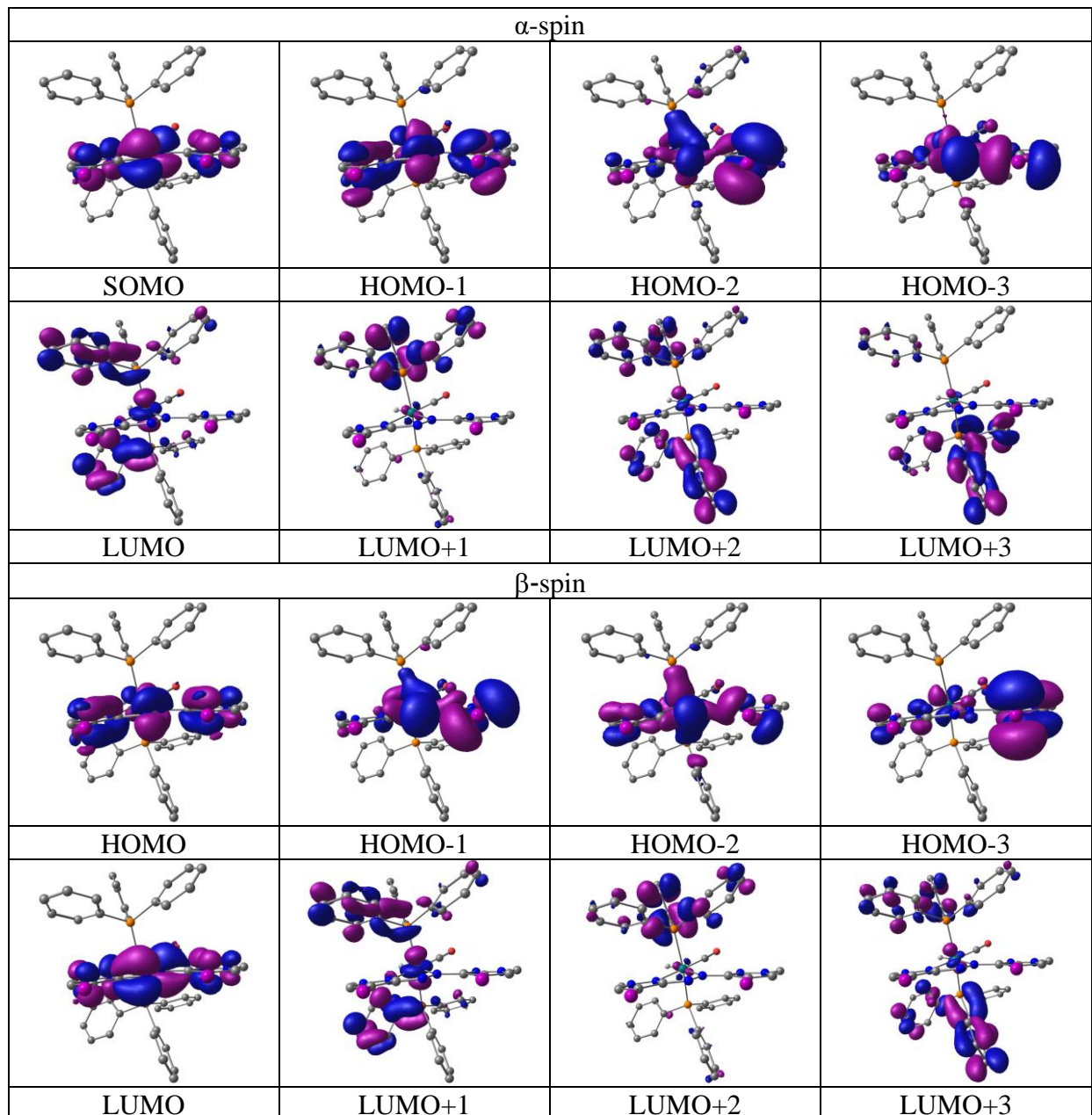


Table S14 Composition and energies of selected molecular orbitals of **2a⁻** ($S = 0$)

MO	Energy(eV)	% Composition				
		Ru	L2	PPh ₃	CO	H
HOMO-5	-2.839	77	10	02	11	00
HOMO-4	-2.762	48	41	05	05	00
HOMO-3	-2.461	49	24	26	01	00
HOMO-2	-2.114	22	70	07	01	00
HOMO-1	-1.911	08	82	04	01	01
HOMO	1.116	13	63	23	01	00
LUMO	1.662	03	03	94	00	00
LUMO+1	1.691	17	09	73	01	00
LUMO+2	1.825	04	01	94	01	00
LUMO+3	2.021	04	04	92	00	00
LUMO+4	2.033	09	02	89	00	00
LUMO+5	2.063	04	02	93	00	00

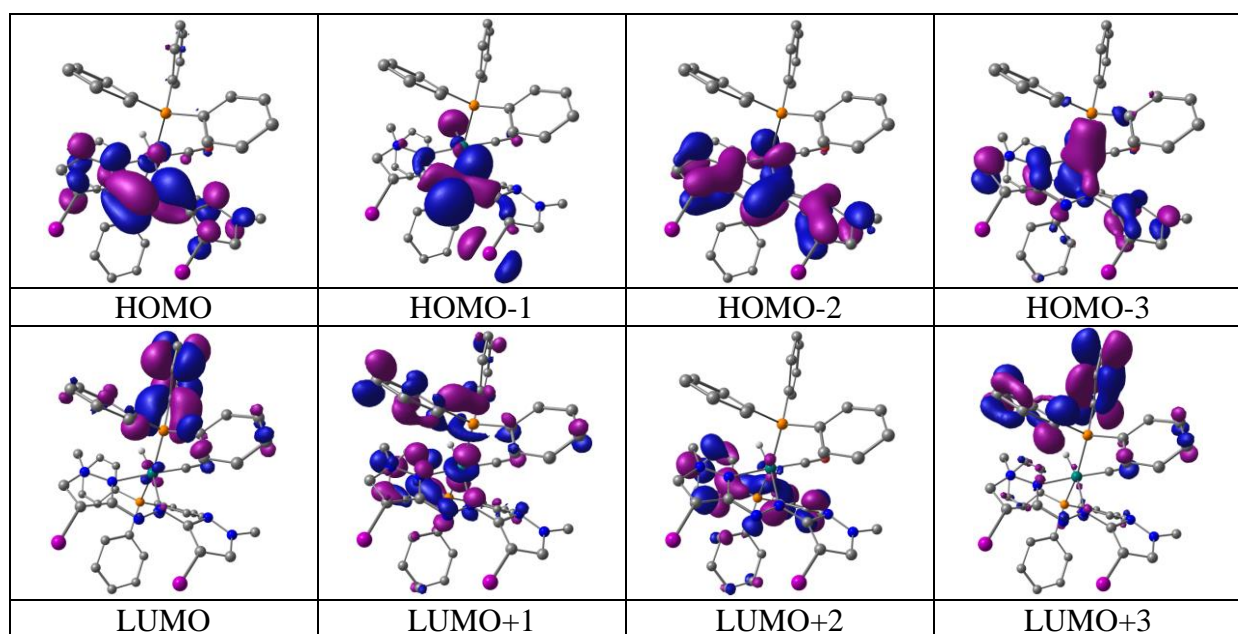


Table S15 Composition and energies of selected molecular orbitals of **2b⁺** ($S = 0$)

MO	Energy(eV)	% Composition				
		Ru	L2	PPh ₃	CO	H
HOMO-5	-8.947	09	12	77	01	00
HOMO-4	-8.893	10	10	79	00	00
HOMO-3	-8.842	13	50	35	02	00
HOMO-2	-8.727	28	24	48	00	00
HOMO-1	-8.529	05	74	20	00	00
HOMO	-8.140	43	13	43	01	00
LUMO	-5.202	07	85	07	01	00
LUMO+1	-3.386	32	08	57	02	00
LUMO+2	-3.261	05	82	12	01	01
LUMO+3	-3.027	06	33	60	01	00
LUMO+4	-2.895	01	92	07	00	00
LUMO+5	-2.889	03	02	92	03	00

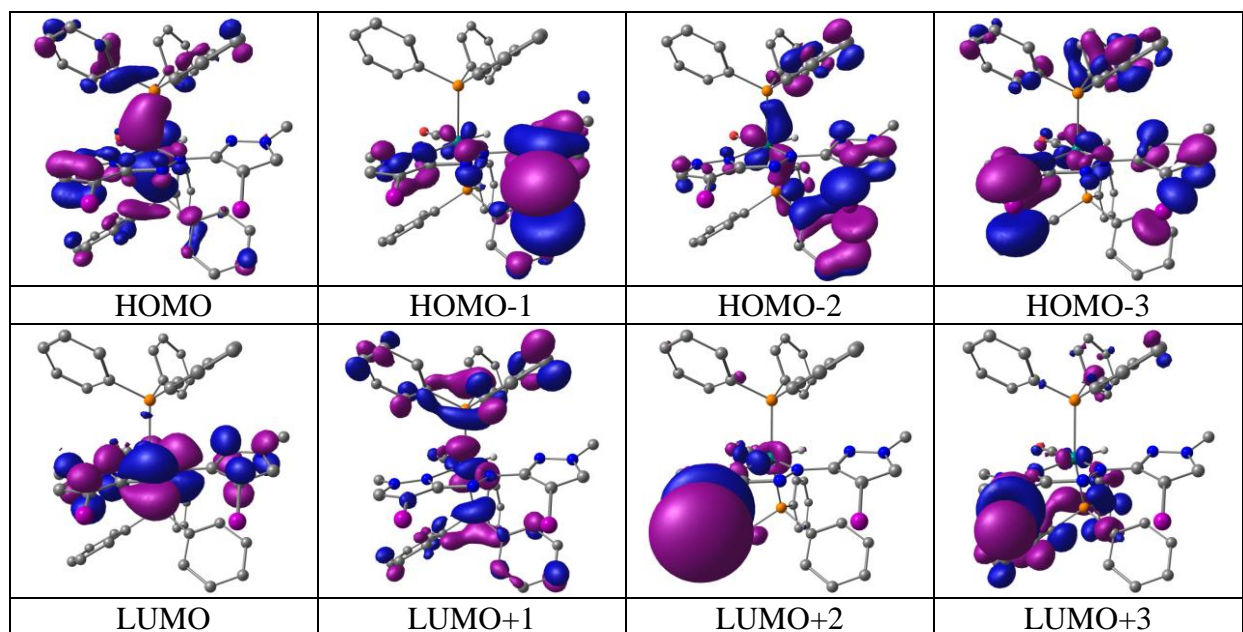


Table S16 Composition and energies of selected molecular orbitals of **2b** ($S = 1/2$)

MO	Energy(eV)	% Composition				
		Ru	L2	PPh ₃	CO	H
α -spin						
HOMO-5	-5.908	79	04	03	14	00
HOMO-4	-5.769	11	82	06	01	00
HOMO-3	-5.572	06	84	06	04	00
HOMO-2	-5.433	06	79	15	00	00
HOMO-1	-5.221	57	23	20	00	00
SOMO	-2.879	06	86	07	01	00
LUMO	-0.813	26	03	70	01	00
LUMO+1	-0.665	05	02	92	01	00
LUMO+2	-0.608	02	01	96	01	00
LUMO+3	-0.479	07	12	81	00	00
LUMO+4	-0.407	02	03	95	00	00
LUMO+5	-0.334	09	04	86	01	00
β -spin						
HOMO-5	-5.974	33	17	48	02	00
HOMO-4	-5.900	80	04	03	14	00
HOMO-3	-5.619	02	95	03	00	00
HOMO-2	-5.400	07	83	06	04	00
HOMO-1	-5.190	41	35	24	00	00
HOMO	-5.067	23	65	11	01	00
LUMO	-0.867	16	46	36	03	00
LUMO+1	-0.782	22	16	60	01	00
LUMO+2	-0.661	05	02	92	01	00
LUMO+3	-0.596	02	04	93	00	00
LUMO+4	-0.469	06	12	81	00	00
LUMO+5	-0.404	02	03	95	00	00

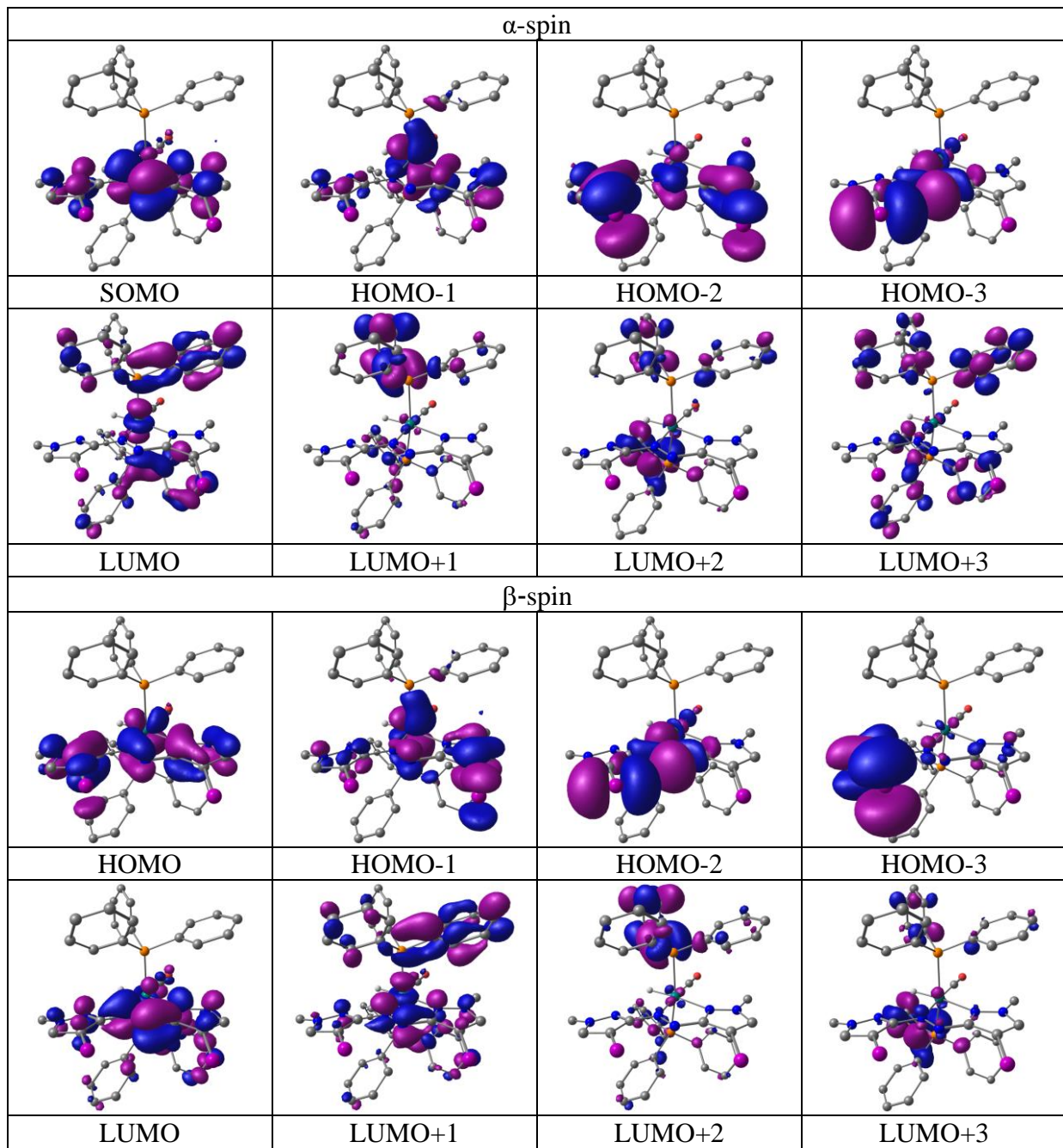


Table S17 Composition and energies of selected molecular orbitals of **2b⁻** ($S = 0$)

MO	Energy(eV)	% Composition				
		Ru	L2	PPh ₃	CO	H
HOMO-5	-2.943	78	06	02	14	00
HOMO-4	-2.901	05	91	03	01	00
HOMO-3	-2.350	42	37	21	00	00
HOMO-2	-2.125	22	67	10	01	00
HOMO-1	-2.074	10	78	07	04	00
HOMO	1.040	10	64	23	02	00
LUMO	1.633	05	03	92	00	00
LUMO+1	1.707	20	02	77	01	00
LUMO+2	1.795	03	03	94	00	00
LUMO+3	1.918	05	05	89	01	00
LUMO+4	2.031	05	03	91	00	00
LUMO+5	2.141	02	03	94	00	00

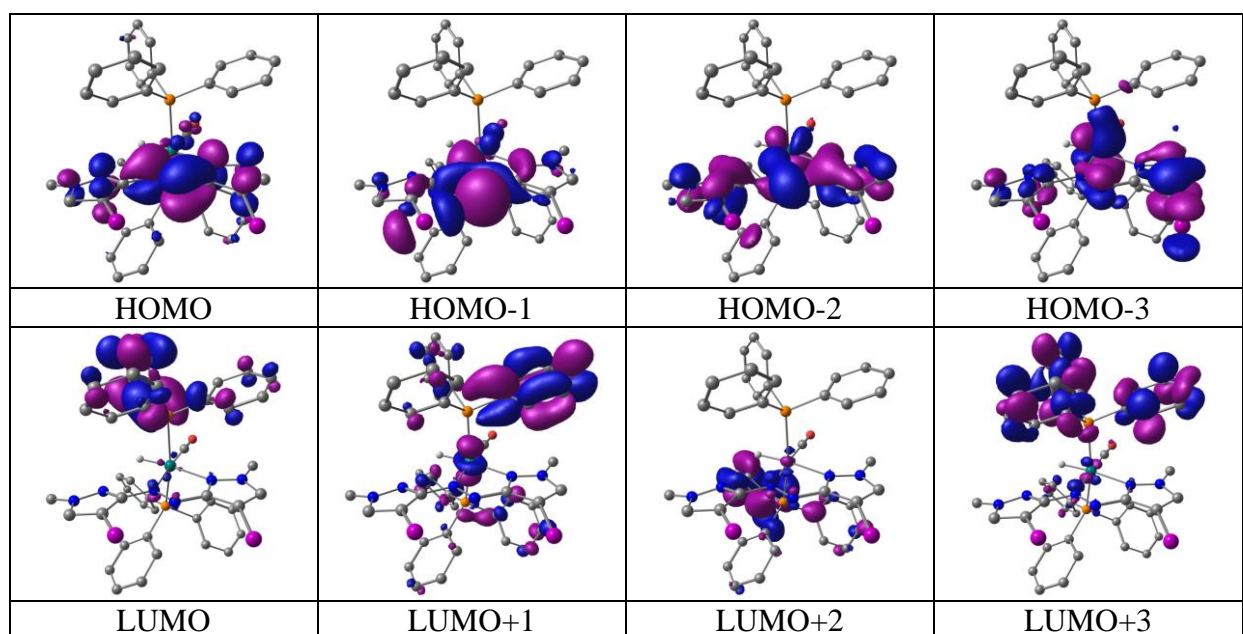


Table S18 Mulliken spin density distributions

Complex	Ru	L1/L2	PPh ₃	CO	H/Cl
1a ($S = 1/2$)	0.014	0.981	0.013	0.002	-0.005
1b ($S = 1/2$)	0.001	0.974	0.012	0.012	-0.002
2a ($S = 1/2$)	0.018	0.972	0.013	0.002	-0.005
2b ($S = 1/2$)	0.003	0.971	0.018	0.011	-0.002

Table S19 Comparison of the electrocatalytic HER

Catalysts	Electrolyte	Overpotential	TOF	FE	Ref.
Co(4,4''-trifluoromethyl-4'-dimethylamino-2,2':6',2''-terpyridine) ₂ ·PF ₆	TBAP/acetic acid	250 mV vs Fc*/Fc	1445 s ⁻¹	-	S3
[{Ni(,2-bis(2-thiabutyl-3,3-dimethyl-4-selenol)benzene)} ₂ Ru(phen) ₂](PF ₆) ₂	TBAPF ₆	640 mV vs Fc*/Fc	-	64%	S4
[{Ni(,2-bis(2-thiabutyl-3,3-dimethyl-4-selenol)benzene)} ₂ Ru(phen) ₂](PF ₆) ₂	TBAPF ₆	650 mV vs Fc*/Fc	-	63 %	S4
[<i>cis</i> -RuCl ₂ (PPh ₃) ₂ (κ ₂ -TL)] (TL = 2-thiophenyl benzimidazole) CH ₃ CN/0.1 M ⁿ Bu ₄ NPF ₆	TFA	-	395 s ⁻¹	-	S5
Cobalt(II)PY ₄	Bu ₄ NPF ₆ , CH ₃ CN, TFA	-	0.011 s ⁻¹		S6
[Co(HBMIMPh ₂) ₂](BF ₄)	Et ₃ NHBF ₄ in DMF	-	555 s ⁻¹	>99%	S7
[Co(bapbpy)Cl] ⁺	ⁿ Bu ₄ NBF ₄ in DMF	890 (±50) mV	110 ± 20 s ⁻¹	93 (±10) %	S8
[Co ^{II} ₂ N,N'-bis(salicylidene)-phenylmethanediamine]	DMF/acetic acid/TBATFB	470 mV	50 s ⁻¹	85–95%	S9
[Co ^{II} Co ^{III} N,N'-bis(salicylidene)-phenylmethanediamine (pyr) ₂] ⁺	DMF/acetic acid/TBATFB	-	1600 s ⁻¹		S9
[Co ^{II} ₂ (NN' ₂ O ₂)(bpy) ₂]ClO ₄	CH ₃ CN/HOAc	-		94 % –1.6 V vs. Ag/AgCl)	S10
[Co ₂ 4-{bis[4-(p-methoxyphenyl)thiosemicarbazone]}-2,3-butane (NCS) ₂]	DMF/Et ₃ NHBF ₄	-	130 s ⁻¹	65% –1.60 V versus Fc ^{+/-}	S11
Co ^{III} ₂ (trpy) ₂ (μ-bpp)(OH)(OH ₂)] ⁴⁺	ⁿ Bu ₄ NPF ₆ in MeCN/HOAc	-	-	79% E= –1.1 V vs SCE	S12
[1a]ClO ₄	0.5 H ₂ SO ₄	263 mV vs RHE	8.27 x 10 ⁻² s ⁻¹	97.4%	This work

References

- S1 A. K. Singh, S. Ji, B. Singh, C. Das, H. Choi, P. W. Menezes and A. Indra, *Mater. Today Chem.*, 2022, **23**, 100668.
- S2 B. Singh, A. K. Singh, A. Priyadarsini, Y.-C. Huang, S. Dey, T. Ansari, S. Shen, G. K. Lahiri, C.-L. Dong, B. S. Mallik and A. Indra, *Chem. Commun.*, 2023, **59**, 6084-6087.
- S3 S. Aroua, T. K. Todorova, V. Mougel, P. Hommes, H.-U. Reissig and M. Fontecave, *Chem. Cat. Chem.*, 2017, **9**, 2099-2105.
- S4 G. Gezer, D. Durán Jiménez, M. A. Siegler and E. Bouwman, *Eur. J. Inorg. Chem.*, 2017, **2017**, 5027-5032.
- S5 V. Kaim, M. Joshi, M. Stein and S. Kaur-Ghumaan, *Int. J. Hydrogen Energy*, 2023, **48**, 30718-30731.
- S6 J. P. Bigi, T. E. Hanna, W. H. Harman, A. Chang and C. J. Chang, *Chem. Commun.*, 2010, **46**, 958-960.
- S7 S. D. de Vos, M. Otten, T. Wissink, D. L. J. Broere, E. J. M. Hensen and R. J. M. K. Gebbink, *Chem. Sus. Chem.*, 2022, **15**, e202201308.
- S8 N. Queyriaux, D. Sun, J. Fize, J. Pécaut, M. J. Field, M. Chavarot-Kerlidou and V. Artero, *J. Am. Chem. Soc.*, 2020, **142**, 274-282.
- S9 T. H. To, D. B. Tran, V. Thi Thu Ha and P. D. Tran, *RSC Adv.*, 2022, **12**, 26428-26434.
- S10 K. K. Kpogo, S. Mazumder, D. Wang, H. B. Schlegel, A. T. Fiedler and C. N. Verani, *Chem. – A Eur. J.*, 2017, **23**, 9272-9279.
- S11 T. Straistari, R. Hardré, J. Fize, S. Shova, M. Giorgi, M. Réglier, V. Artero and M. Orio, *Chem. – A Eur. J.*, 2018, **24**, 8779-8786.
- S12 S. Mandal, S. Shikano, Y. Yamada, Y.-M. Lee, W. Nam, A. Llobet and S. Fukuzumi, *J. Am. Chem. Soc.*, 2013, **135**, 15294-15297.